Palaeogeography, Palaeoclimatology, Palaeoecology 640 (2024) 112101

Contents lists available at ScienceDirect

Palaeogeography, Palaeoclimatology, Palaeoecology

journal homepage: www.elsevier.com/locate/palaeo

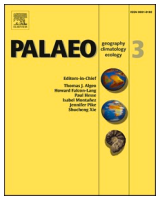

Molecular and mineral biomarker record of terrestrialization in the Rhynie Chert

T.O. Akinsanpe [a,b], S.A. Bowden [a], J. Parnell [a,*]

[a] School of Geosciences, University of Aberdeen, Aberdeen AB24 3UE, United Kingdom
[b] Obafemi Awolowo University, Ile Ife 220103, Osun State, Nigeria

ARTICLE INFO

Keywords:
Devonian
Rhynie basin
Organic geochemistry
Biomarker
Fossil plants

ABSTRACT

The colonization of the terrestrial surface by land plants involved the evolution of a complex ecosystem of plants, animals, fungi, algae and bacteria, within a mineral framework. The record of this advance is highly fragmentary and uncertain. However, a wealth of fossil evidence is preserved in the Lower Devonian Rhynie Chert lagerstätte, which is consequently considered to be the world's oldest preserved terrestrial ecosystem. The physical record of fossils in the Rhynie Chert is accompanied by a chemical record of molecular biomarkers and mineral diagenesis. The biomarkers include components derived from vascular and other higher plants, and decomposers fungi and bacteria. The chert contains the earliest record of the plant diterpane *ent*-beyerane, identified in this study. The biomarker profile is distinct from that in Lower Devonian organic-rich shales at Strathpeffer, 100 km to the west, where plants are not preserved and the environment was hypersaline. In addition to organic biomarkers, the chert contains mineralogical characters which imply biological activity, including pyrite framboids, strongly leached monazite and garnet, and pitted micas similar to grains altered by modern fungi. The molecular and mineral biomarkers combine with the fossil record and phylogenetic data in the toolbox available to document plant colonization and symbiosis on the terrestrial surface.

1. Introduction

The world's oldest preserved terrestrial ecosystem is in the 407-million-year-old (Lower Devonian: Pragian-Emsian) Rhynie Chert (Fig. 1), a lagerstätte of early plants and their accompanying biota of cyanobacteria, green algae, fungi, arthropods etc. (Strullu-Derrien et al., 2014; Trewin and Fayers, 2015; Edwards et al., 2018; Wellman et al., 2019). The early evolution of plants was tied to the occurrence of fungi, with which they developed in symbiosis (Strullu-Derrien et al., 2014; Lutzoni et al., 2018). The chert beds at Rhynie contain plants (Figs. 2, 3) with remarkably preserved cells, in which, despite silicification, primary carbon is preserved (Abbott et al., 2017; Loron et al., 2023). Combined with only a limited burial history, and therefore minimal thermal alteration (Rice et al., 2002), the cherts are a viable source of biomarkers which could represent the components of the ecosystem.

Several plants are distinguished in the chert (Trewin, 1994; Trewin and Fayers, 2015). There are multiple interpretations of their phylogeny, but a broad division can be made between true vascular plants (*Asteroxylon, Rhynia*), and less complex pre-vascular plants (*Aglaophyton, Nothia*, *Horneophyton*). The chert beds include plants in upright growth position, dominated by forms that are considered to be vascular plants (Cascales-Miñana et al., 2019), and laminae of organic matter which are composed of phytodebris (plant cuticles etc.) together with cyanobacteria (Fig. 2; Trewin and Fayers, 2015, Strullu-Derrien et al., 2023). The non-photosynthesizing fraction of organic matter would include a range of microbial matter including archaea and bacteria, which dominate many modern hot spring systems and consume or liberate gases including methane and hydrogen (Gomez, 2011; Escuder-Rodríguez et al., 2022), but which are not evident in petrographic studies. Organic matter also occurs in interbedded grey shales which represent an ephemeral lacustrine environment. Several types of fungal interaction with plants have been documented in the Rhynie Chert (Powell et al., 2000; Taylor et al., 2004; Strullu-Derrien et al., 2014; Krings et al., 2018).

Further data for the Lower Devonian terrestrial ecosystem can be measured in organic-rich shales found 100 km to the west of Rhynie at Strathpeffer. The organic-rich shales from Strathpeffer share a low thermal maturity with Rhynie sediments and their proximity implies a similar climate and continentality. However, deposits from Strathpeffer lack megascopic plant fossils, although they contain plant spores.

* Corresponding author.
E-mail address: J.Parnell@abdn.ac.uk (J. Parnell).

https://doi.org/10.1016/j.palaeo.2024.112101
Received 3 October 2023; Received in revised form 8 February 2024; Accepted 16 February 2024
Available online 19 February 2024

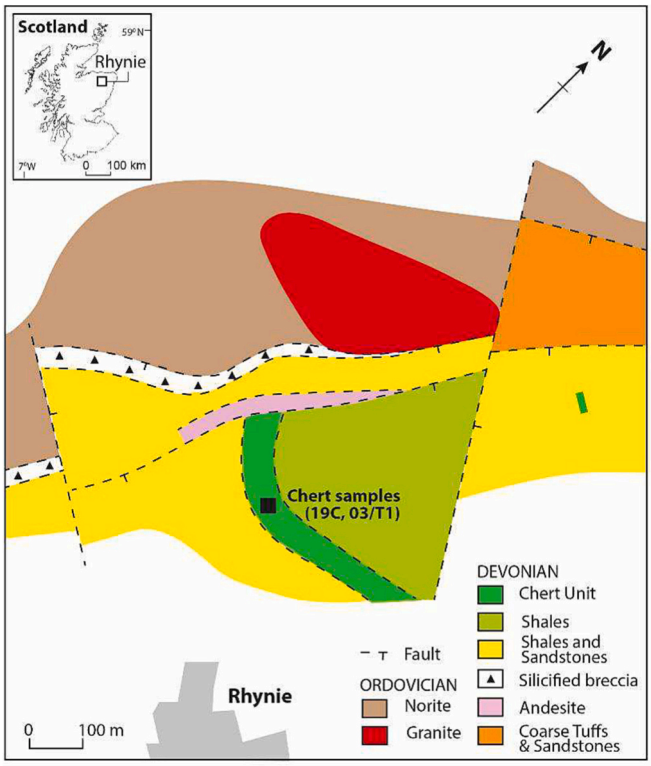

Fig. 1. Geological map of region near Rhynie village (after Rice et al., 2002).

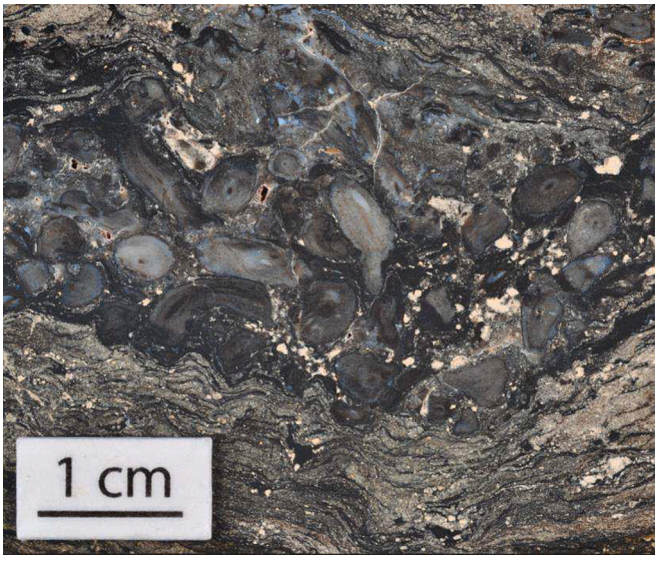

Fig. 2. Main facies in Rhynie Chert. Contrast between plant-bearing chert (centre) and laminae of phytodebris with intermixed sand and authigenic oxide minerals (lower). Note phytodebris not penetrated by roots.

Together, the Lower Devonian deposits at Rhynie and Strathpeffer allow testing for biomarkers of the Lower Devonian terrestrial ecosystem, and particularly between a unit with a life assemblage of plants and related biota, and one without.

The distribution of organic biomarkers in terrestrial sedimentary rocks helps to delineate the evolution of land plants (Versteegh and Riboulleau, 2010; Böcker et al., 2013). In the pre-angiosperm evolutionary scheme, tetracyclic diterpenoids are particularly valuable. These compounds, including *ent*-kaurane, *ent*-beyerane and phyllocladane, are relatively stable, so have become established as biomarkers, attributed

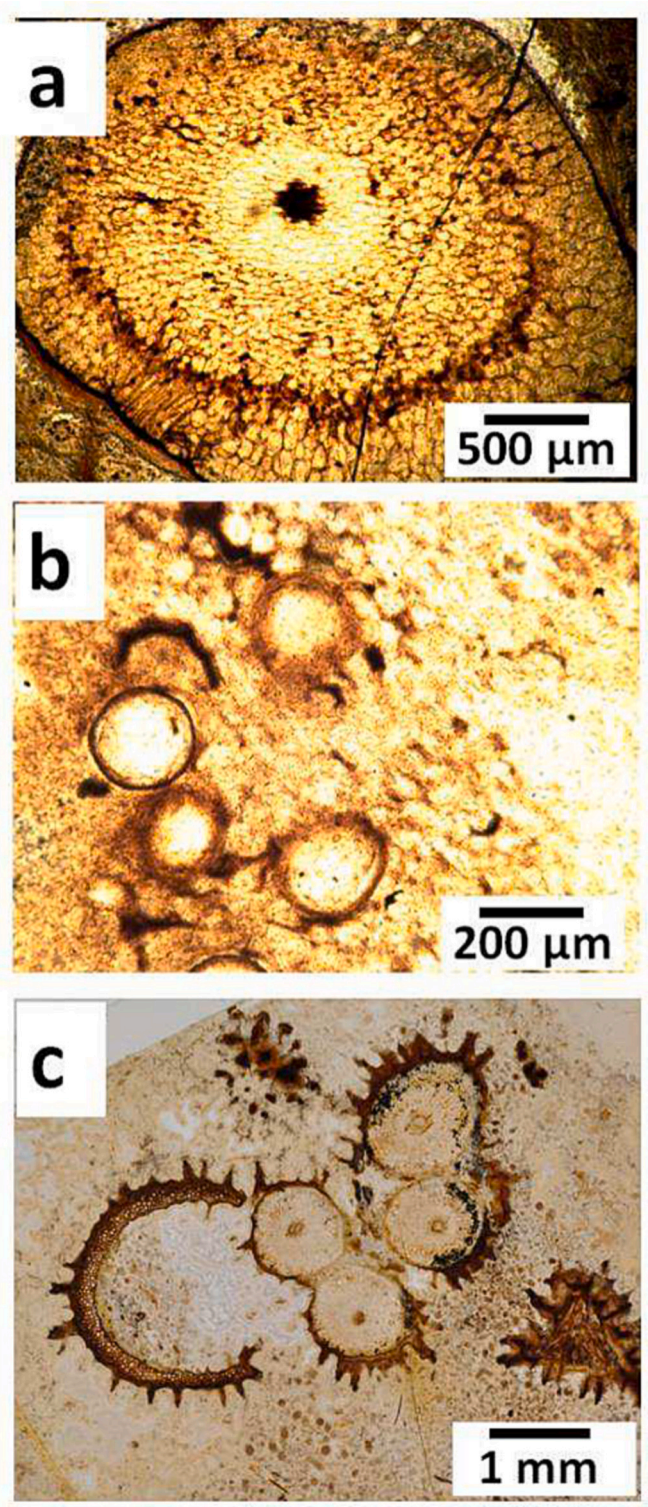

Fig. 3. Thin section micrographs of Rhynie Chert and associated Windyfield Chert, showing brown-coloured kerogen. A, Fungal ring (dark brown) within plant stem, Trench 03/T1Chert bed 9; B, Fungal cysts within plant stem, Trench 03/T1 Chert bed 9; C, Cynanobacterial crusts on plant fragments, Windyfield Chert float sample RW20. (For interpretation of the references to colour in this figure legend, the reader is referred to the web version of this article.)

to synthesis from abietic acid in conifers and earlier vascular plants (Noble et al., 1985; Romero-Sarmiento et al., 2011).

Only exceptionally have fossil fungi in symbiosis with plants survived, but where early permineralization has preserved fungi, they may

yield a molecular record. Biomolecular evidence for fungi in the geological record has focussed on the polyaromatic hydrocarbon perylene (Grice et al., 2009; Marynowski et al., 2013), which is documented as a fungal biomarker back to the end-Permian. Recent data, however, suggests that perylene can have a more diverse origin, including plant pigmentation and diagenesis (Li et al., 2022). Perylene is also found in modern marine/lacustrine sediments, washed off land surfaces, and by analogy perylene-bearing shales back to the Middle Devonian have been interpreted to signify a terrestrial hinterland (Tulipani et al., 2015; Philp and De Garmo, 2020). Notwithstanding the uncertainty in interpretation, these observations indicate that perylene survives from the Devonian and could be found in the Rhynie Chert.

The sedimentary host/template is a fundamental part of the ecosystem, with which biological components can interact. The Devonian Rhynie Chert is ideal for study of such interaction in the geological record. Plants, fungi and minerals are well preserved by contemporaneous silicification, hot spring siliceous fluids introduced anomalous amounts of trace elements to the environment, and the deposit has not been overprinted by later geological events or high temperatures. Fungi particularly provide phosphorus to plants as part of their symbiotic relationship. Several minerals are targeted by fungi in the modern environment, to enable associated plants to obtain specific elements. Examples include the extraction of phosphorus, potassium and magnesium from monazite, feldspars and amphiboles respectively (Hoffland et al., 2003; van Schöll et al., 2006; Lian et al., 2008; Kang et al., 2021). Some micas localize fungal activity, especially if they are potassium-bearing, such as muscovite (e.g. van Schöll et al., 2006; Quirk et al., 2012; Song et al., 2015). Fungal extraction of lithium from the mica lepidolite is also recorded (Sedlakova-Kadukova et al., 2020). White (potassic) micas are abundant in beds of phytodebris in the Rhynie Chert (Trewin and Fayers, 2015), which also contain remains of fungi (Powell et al., 2000), so the mica was targeted for study.

The potential of the biomarker record in the Rhynie Chert is evaluated here, in particular to determine:

(i) If molecular biomarkers can be resolved to represent different components of the ecosystem, especially plants and fungi.
(ii) Identification of petrographic evidence for a biological role in mineral precipitation, in which fungal activity is likely to be important.
(iii) Whether the biomarker distribution in Rhynie and Strathpeffer sediments is consistent with differences in environment in these two Lower Devonian sections.

2. Geological setting

The Rhynie Chert occurs in the Rhynie Basin, northern Scotland, a half-graben with a basin-fill of continental Lower Devonian (Lower Old Red Sandstone; LORS) sedimentary and volcanic rocks (Rice et al., 1995; Trewin and Fayers, 2015). Palynology indicates a Pragian to earliest Emsian age (Wellman, 2006). Lacustrine shales and sandstones of the Dryden Flags Formation host the Rhynie Chert, an ephemeral pool with hot springs within a geothermal wetland (Rice et al., 2002; Trewin and Fayers, 2015). The chert preserved the earliest terrestrial ecosystem comprising vascular plants, fungi, macro-algae, aquatic and terrestrial animals, which were buried by silica-rich waters from hot-spring vent pools (Trewin and Fayers, 2015). The chert consists of variable combinations of two main facies; plant-bearing silica sinter which may be in growth position, and layers of compacted phytodebris mixed with detrital sediment up to sand grade (Fig. 2). A separate silicified body, the Windyfield Chert, lies 700 m to the north-east of the Rhynie Chert, and represents a distinct centre of hydrothermal activity (Fayers and Trewin, 2004). The biota of the two cherts is very similar, and they were penecontemporaneous. The Windyfield Chert is a few hundred metres higher in the succession than the Rhynie Chert (Rice and Ashcroft, 2004).

Previous observations of organic matter in the Rhynie Chert were focussed on samples from boreholes and trenches adjacent to the fault bounding the Devonian basin (Rice et al., 2002), and recorded relatively high thermal maturity, including blackened palynomorphs (Rice et al., 1995; Wellman, 2006). This probably reflects the channelling of hot mineralizing fluids through the fault zone (Baron et al., 2004). The current study is based particularly on samples from a trench excavated in 2003, more distant (about 300 m) from the fault (Fig. 1), in which the organic matter is coloured brown (Fig. 3) and hence holds a higher potential for the determination of biomarkers. Samples containing light brown kerogen also from the nearby Windyfield Chert (Fig. 3) confirm that the ambient maturity is suitable to yield biomarkers.

The organic-rich shales at Strathpeffer are slightly younger, from middle to late Emsian (Richardson and Rasul, 1978). They accumulated in a half-graben, as at Rhynie, but the shales passed laterally into a thick sequence of conglomerates banked against the boundary fault (Clarke and Parnell, 1999). While the bounding fault at Rhynie channelled mineralizing fluids during sedimentation, the fault at Strathpeffer did so at a later stage after sediment lithification (Parnell et al., 2016). Also as at Rhynie, the Strathpeffer sediments were partly chertified pre-compaction, by silicification of gypsum, and were additionally per-mineralized by dolomite (Parnell, 1985). Abundant sulphate evaporites associated with the organic-rich shales led to pyrite precipitation in the shales (Parnell, 1985). Long-term generation of waters rich in hydrogen sulphide from the pyritic shales led to the establishment of Strathpeffer as a spa town focussed around the outcrop of shales (Manson, 1879; Fox, 1889).

The sandstones in the Rhynie Chert contain quartz, feldspar, mica and chloritoid grains, with minor amounts of heavy minerals zircon, monazite, ilmenite and garnet. The monazite and zircon are derived from erosion of Caledonian granites. Many of the sandstones are highly micaceous, which reflects their derivation from Dalradian (Neoproterozoic) metasediments dominated by micaceous schists, and deposition in low-energy fluvial settings (Trewin and Fayers, 2015). White micas are predominantly muscovite, but with variable composition. Micas in the parent Dalradian schists had been variably altered to phengite, with variable composition in individual crystals, during the Caledonian Orogeny (Dempster, 1992; Aoki et al., 2013), and these variable compositions are therefore expected in the derived Devonian sediments. Biotite micas in Caledonian granite in the region are also variable altered to phengitic muscovite (Harrison, 1990). The whole rock at Rhynie was silicified as part of the chert formation that affected the whole deposit.

3. Methods

Sampling. Samples were sourced from archives in the School of Geosciences, University of Aberdeen. They consist of three spatially associated suites: a trench (03/T1; Fig. 1) through bedrock excavated in 2003, loose blocks lying on the bedrock in the trench, and a borehole (19C) drilled in 1988. Each suite is preserved with depth data. All samples were originally collected responsibly, and according to local laws. Eleven distinct beds of the Rhynie Chert from trench 03/T1, and four grey shales representing an ephemeral lacustrine environment from borehole 19C, were sampled. The trench and borehole samples are linked by very close proximity (Fig. 1) and the occurrence of plant-bearing cherts in both. Samples were selected from borehole 19C depths 12.0 m, 14.7 m, 17.0 m, 17.2 m, 17.3 m and 19.4 m because petrographic study (Powell et al., 2000) identified them as well-colonised by fungi. A sample of andesite from borehole 97/8, archived with the cherts, was analysed to test that no modern fungal signal was present. Fifty samples of Rhynie Chert dominated by either plants or laminae of phytodebris were drilled to produce powders. Nine samples of near-coeval shales from Strathpeffer were also sampled. Before drilling, the rock samples were treated with dichloromethane (DCM) followed by distilled water to eliminate any weathering effects on their surfaces or associated contamination.

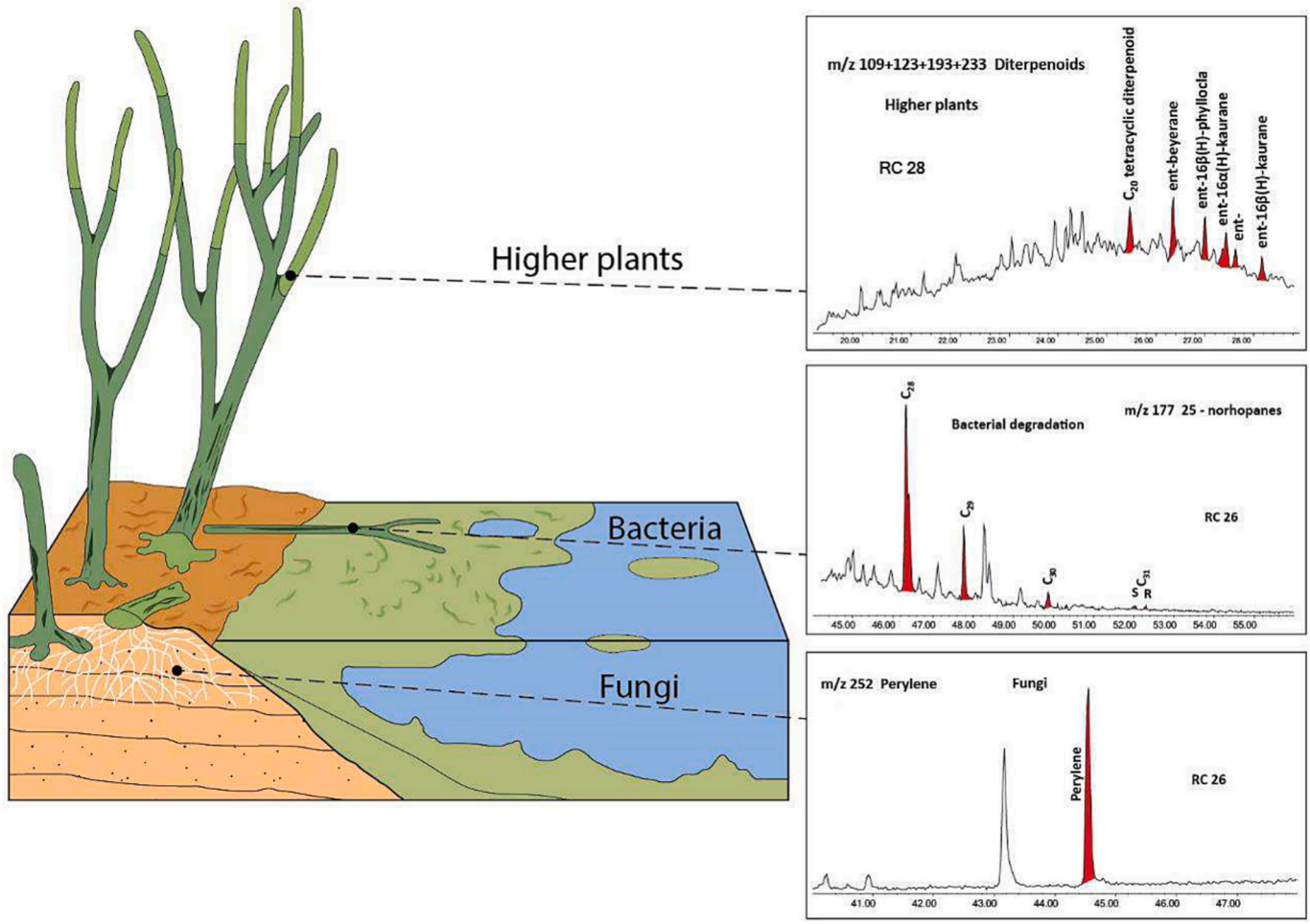

Fig. 4. Schematic environment of Rhynie Chert, distinguishing biomarkers for specific components. Chromatograms from this study highlight diagnostic peaks (red) in numbered samples. Schematic re-designed from N.H. Trewin (unpublished) and Strullu-Derrien et al. (2021). (For interpretation of the references to colour in this figure legend, the reader is referred to the web version of this article.)

Elemental Analysis. The total organic carbon (TOC) values were determined on 200 mg of powdered decarbonated samples using the LECO CS744 Carbon Sulphur Analyser at the University of Aberdeen. The decarbonisation process was done by treating the samples with 20% and 10% hydrochloric acid (HCl) several times until there was no effervescence. This was used to remove the inorganic carbon present in the samples in the form of gases such as CO_2.

Biomarker measurement. The biomarker extractions were achieved with DCM/methanol (MeOH) (9/1, *v*/v) using a DIONEX Accelerated Solvent Extractor (ASE-200) and micro-extraction method (ME) for sample masses <0.3 g. The micro-extraction process involved adding 10 ml of DCM and MeOH mix (1/1, v/v) to the weighed sample in a vial. This was mixed and placed in the ultrasonic bath for 15 min. The resulting solvents were then transferred into clean vials with a pipette. These steps were repeated with a solvent mix of DCM and MeOH (3/1, v/v) and 100% DCM. The dried extracted organic matter (EOM) from ASE and ME was separated into aliphatic, aromatic, and polar fractions by silica column chromatography using hexane, hexane/DCM (3/1, v/v), and DCM/MeOH (2/1, v/v), respectively. The glassware used was thoroughly cleaned with a 93:7 mixture of DCM/ MeOH. This paper only focuses on the saturate and aromatic hydrocarbon fractions.

Analysis used an Agilent 6890 N gas chromatograph fitted with a J&W DB-5 phase 50 m MSD and a quadrupole mass spectrometer operating in scan and selected ion monitoring (SIM) mode (dwell time 0.1 s per ion and ionisation energy 70 eV). The samples were injected manually using a split/splitless injector operating in splitless mode (purge 40 ml min^{-1} for 2 mins). The temperature programme for the GC oven was 80–295 °C, holding at 80 °C for 2 mins, rising to 10 °C min^{-1} for 8 mins and then 3 °C min^{-1}, and finally holding the maximum temperature for 10 min^{-1}. Quantitative biomarker data were obtained for both saturate and aromatic fractions. These include n-alkanes and acyclic isoprenoids, measured on the charge-to-mass ratio (*m/z*) 85; tetracyclic diterpenoids (*m/z* 109, 123, 193 and 233); β-carotane (*m/z* 125); norhopanes, hopanes and methylhopanes (*m/z* 177, 191 and 205); and steranes (*m/z* 217 and 218). The aromatic compounds were measured on *m/z* 183, 202, 219 and 252, including cadalene, pyrene, retene and perylene, respectively. Mass spectra for diterpenoids, norhopanes, cadalene and retene are shown in Figs. S2, S3, S4 and S5. The different tetracyclic diterpenoids were monitored on a combined *m/z* 109 + 123 + 193 + 233 chromatogram. The peaks were identified by comparing their mass spectra and retention times with available published data for well-characterized samples from Romero-Sarmiento et al. (2011; Figs. S1, S2)) and Noble et al. (1985). A sample of SKT-D from the 2011 study was run with our samples. A standard for perylene (>99% purity), was obtained from Sigma Aldrich. Thermal maturity was estimated from the 20S/20S + 20R ratio for C_{29} sterane, based on the P stereoisomeric transformation and the corresponding increase in the proportion of the S isomer with maturation (Peters et al., 2005). The gammacerane index was calculated as the ratio of gammacerane/(gammacerane + C_{30} hopane). The concentration of all compounds is reported relative to the internal standard of 5β-cholane, with the response of 5β-cholane measured on the *m/z* 217 ion chromatogram.

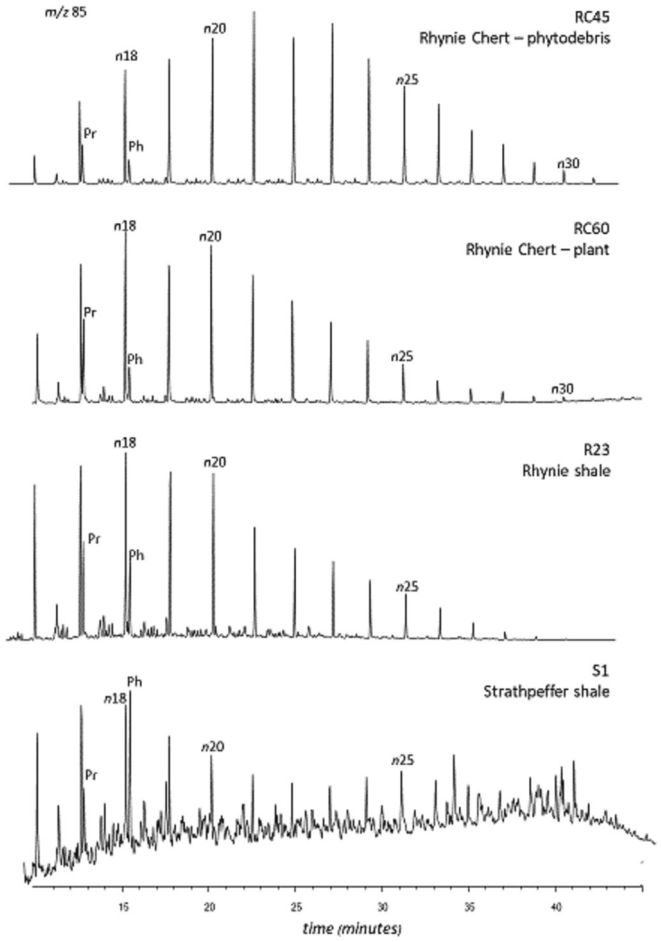

Fig. 5. Mass chromatograms *m/z* 85 of aliphatic fractions for plant and phytodebris beds. Distribution of n-alkanes and acyclic isoprenoid hydrocarbons (pristane Pr, phytane Ph) shown from samples of Rhynie Chert, and shales at Rhynie and Strathpeffer for comparison. Plant-bearing bed has higher Pr/Ph ratio than phytodebris bed.

The sample extracts are preserved frozen in the Organic Geochemistry Laboratory, School of Geosciences, University of Aberdeen.

Raman Spectroscopy. A Renishaw inVia reflex Raman spectrometer was used for micro-Raman analyses, with a backscattering geometry in the range of 700–3200 cm^{-1} (first- and second-order Raman spectra), with a 2400 1 mm^{-1} spectrometer grating and CCD detector under a maximum of ×100 optical power (numerical aperture (NA) of the lens of 0.90). The slit opening was 65 μm with CCD area of c. 10 pixels (80% of the total signal height hitting the CCD chip) and a confocal hole of 200 μm. A 514.5 nm diode laser was used for excitation with an output of 50 mW. Optical filters (1%) were used to adjust the power of the laser to <0.5 mW. Raman backscattering was recorded after an integration time of 20 s for three repetitions for each measurement. The Raman system was calibrated against the 520.7 cm^{-1} band of silica.

Electron Microscopy. Scanning electron microscopy (SEM) was conducted in the Aberdeen Centre for Electron Microscopy, Analysis and Characterisation (ACEMAC) facility at the University of Aberdeen using a Carl Zeiss Gemini SEM 300 VP Field Emission instrument equipped with an Oxford Instruments NanoAnalysis Xmax80 Energy Dispersive Spectroscopy (EDS) detector, and AZtec software suite. Imaging was done in backscattered mode. Standards were supplied by the factory. Samples were polished using corundum and alumina pastes, cleaned with ethanol, then carbon-coated.

4. Results

4.1. Molecular biomarker preservation

At both Rhynie and Strathpeffer, permineralization pre-compaction preserved the organic matter and a high-resolution suite of biomarkers (Tables S1, S2). The 20S/20S + 20R ratio for the C_{29} sterane is in the range 0.45 to 0.65 which indicates the upper part of the oil window. The plant-bearing beds and phytodebris beds (Fig. 2) have mean organic carbon contents of 0.36% (n = 26) and 0.77% (n = 22) respectively. Consequently, we can decipher the organic components to a degree exceptional in rocks of Lower Devonian age. Measurements focussed on biomarkers for specific components of the ecosystem (Fig. 4), including higher plants (cadalene, diterpenoids), fungi (perylene??) and biodegradation most likely attributable to bacteria (25-norhopanes). Quantitative data are calculated based on identifications of peaks for *n*-alkanes/isoprenoid hydrocarbons (Fig. 5),diterpenenoids (Fig. 6), steranes and hopanes (Fig. 7). Summary plots for pristane/phytane ratios, steranes, hopanes, perylene, and gammacerane indices (Fig. 8) show how the compositions of plant-bearing beds and phytodebris beds compare. A ternary plot of C_{27}, C_{28} and C_{29} steranes (Fig. 9) shows that the plant and phytodebris samples have a comparable sterane composition, but Rhynie shale samples (n = 4) are relatively enriched in the C_{27} sterane, while the Strathpeffer shale samples (n = 9) are relatively lacking in the C_{27} sterane. Changes in the diterpenoid distribution through trench 03/T1 are shown in Fig. 10.

4.2. Raman spectroscopy

Measurements on carbon in Rhynie Chert samples converted to vitrinite reflectance values (Ro %) using the approach of Schito and Corrado (2020) yield a range of maturities from 0.63 to 1.21% (Table S3). Omitting two outliers of data (0.63, 1.21), the data range from 0.80 to 1.10%, with a mean value (n = 20) of 0.93 ± 0.10%. The median value is also 0.93%.

4.3. Sediment mineralogy

Several minerals in the phytodebris layers exhibit alteration, including monazite, garnet and mica. Detrital monazite grains show dissolution pits and reprecipitation (Fig. 11) and detrital garnet also shows dissolution pits (Fig. 11). The garnet grains typically contain several percent manganese. The alteration in heavy mineral grains in the chert is not observed in sandstones in the same succession.

The most abundant altered minerals are silicified micas. The micas exhibit numerous holes, typically 2 μm diameter (Fig. 12). The holes are present in both polished and unpolished samples. Some mica grains show layers of different composition, alternating between ideal muscovite and altered muscovite. The ideal muscovite contains no or few holes, while the altered muscovite has many holes. The margins of many holes are brighter in SEM images. Analyses of the host mica show higher contents of sulphur (up to 2%) in the bright rim, in contrast to the background mica (usually no sulphur, rarely up to 1%). The grains have neoformed mineral precipitates on their surfaces, including titanium-iron oxides and monazite.

The chert is extensively mineralized by pyrite framboids (Fig. 11), and also clusters of pyrite microcrystals with a less organized morphology. The Rhynie framboids are commonly arsenic-rich, and in some samples they are manganese-rich.

5. Discussion

5.1. Thermal maturity

The thermal maturity of the Rhynie Chert samples is indicated by several lines of evidence. The kerogen is brown (Fig. 3), distinct from the

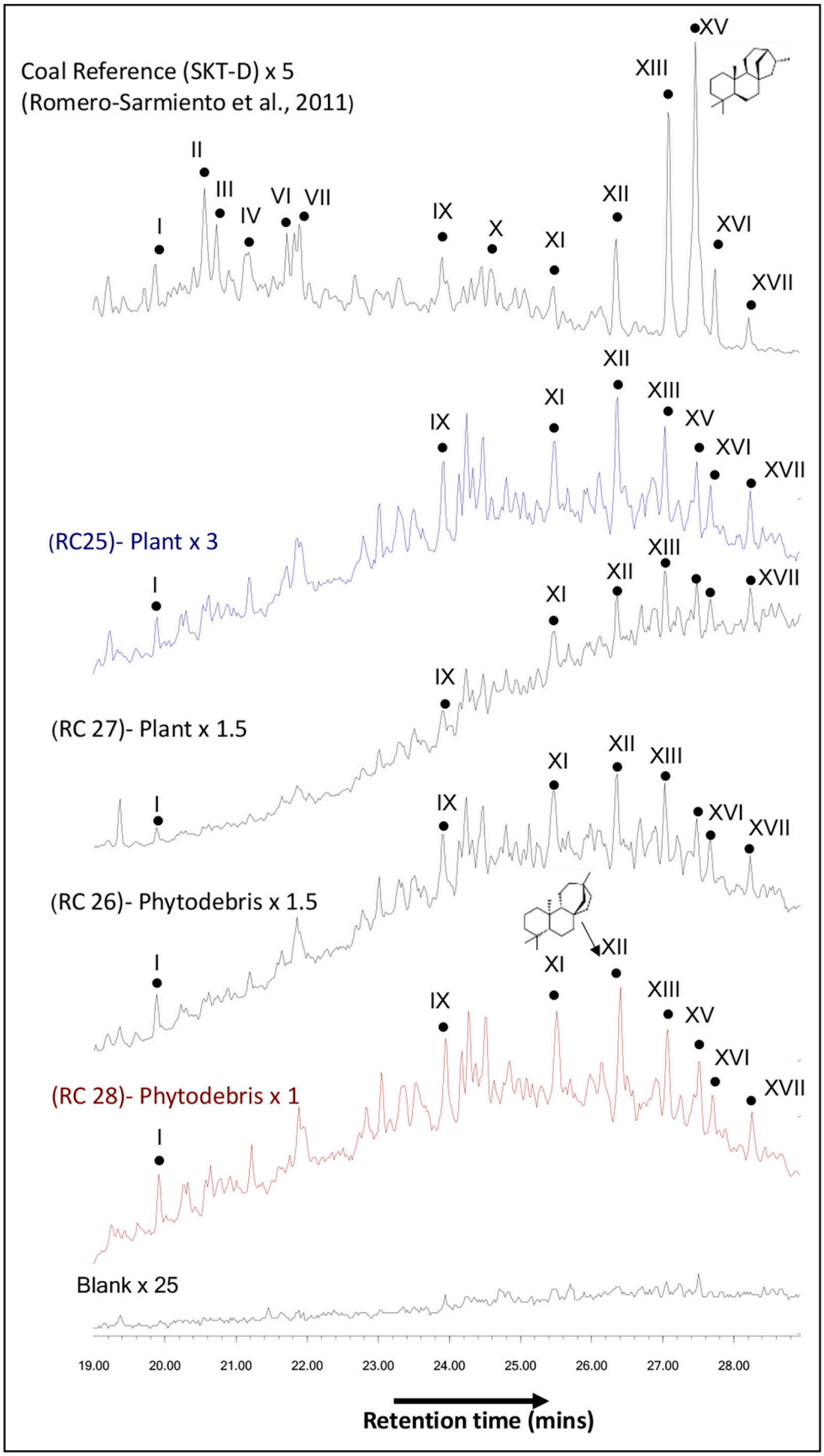

Fig. 6. Summed m/z 109 + 123 + 193 + 233 chromatograms showing diterpenoid distribution in selected Rhynie samples. Peak XII represents *ent*-beyerane. Peak XV represents *ent*-16α(H)-kaurane. Peak identifications are in Table S2. The mass spectra and retention time of peaks of studied samples were compared with that of reference sample SKT-D in Romero-Sarmiento et al. (2011).

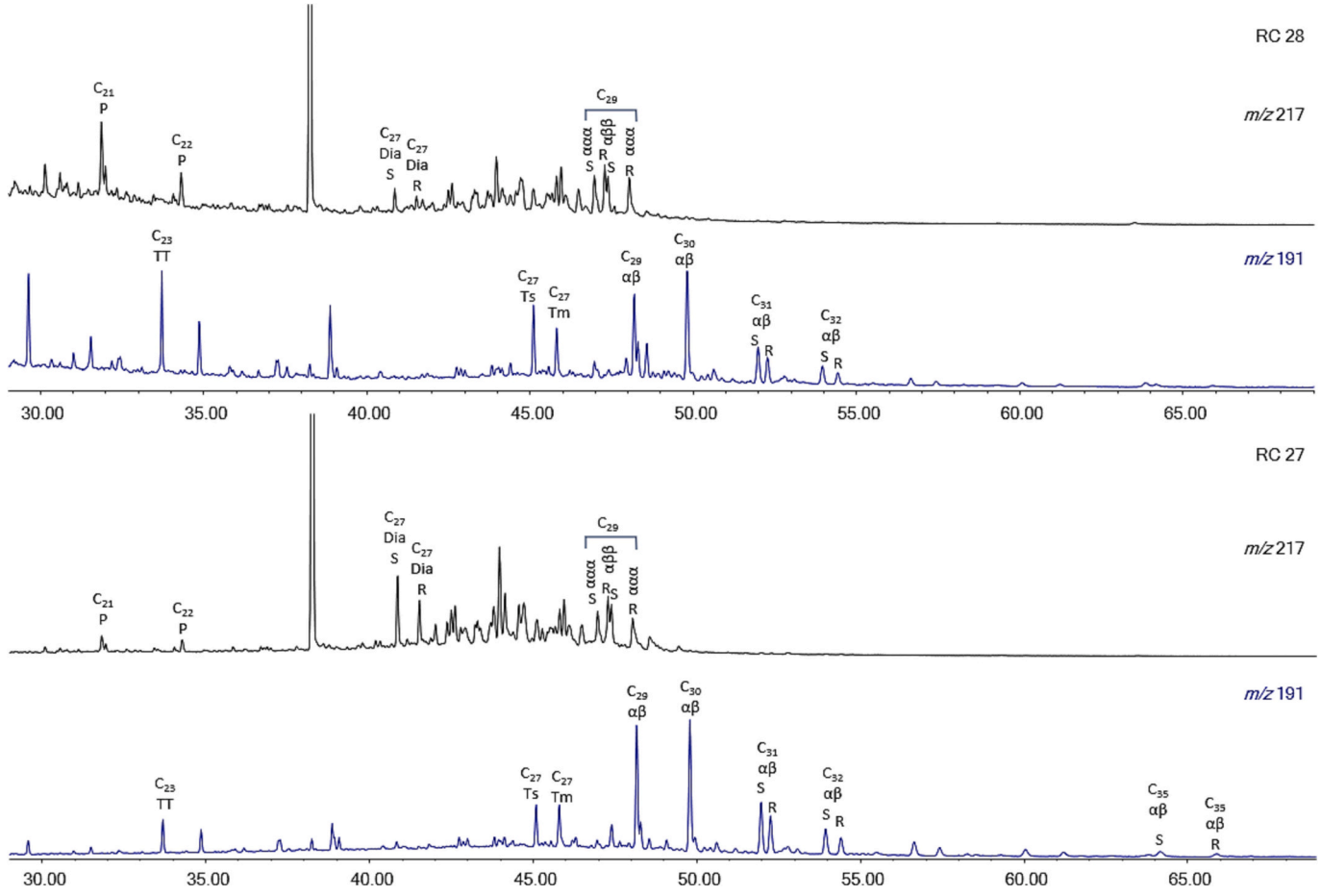

Fig. 7. m/z 217 and 191 ion chromatograms for samples RC28 and RC27. C21P and C22P = C21 and C22 pregnane; C27 Dia S and R = C27 13β,17α(H) 20S and 20R diasterane; C29 ααα S = C27 5α,14α,17α(H) 20S sterane; C29 αββ R = C27 5α,14β,17β(H) 20R sterane; C23TT = C23 13β,14α(H) tricyclic terpane; C27Ts = C27 18α(H)-22,29,30-trisnorneohopane; C27Tm = C27 17α(H)-22,29,30-trisnorhopane; C30 αβ = C30 14α,17β (H) hopane, C31 αβ R = C31 14α,17β (H) 22R hopane.

blackened samples examined by Wellman (2006) from adjacent to the fault zone.

Carbon Preference Index (CPI) values are near-unity (Table S1), typical of oil window conditions. The sterane isomerization values (Table S1) are near-maximum, characteristic of upper oil window conditions. Raman spectroscopy of carbon in the samples, converted to vitrinite reflectance (Table S3), yields a mean Ro value of 0.93%, also characteristic of the upper oil window.

The maturity achieved reflects hydrothermal heating, as shown by the greater maturity increase in the fault zone. This rapid heating is distinct from thermal maturity due to burial, and may have allowed greater preservation of biomarkers for a given reflectance value (Rabinowitz et al., 2017; Savage et al., 2018). For example, perylene is present in coal tar and wood pyrolysis products (Cook et al., 1933), so is known to survive short term high-temperature heating of the kind found in hydrothermal systems.

Notwithstanding the nature of the heating, previous studies show that thermal maturities up to Ro 1% can preserve abundant biomarkers (Dzou et al., 1995), and they imply that the Rhynie Chert has a good potential for biomarker data.

Pyrene occurs in many Rhynie Chert samples (Figs. S6, S7), in common with other sedimentary rocks containing organic matter, at a wide range of thermal maturities (Fang et al., 2015).

5.2. Molecular biomarkers

5.2.1. n-alkanes and isoprenoids

The proportions of *n*-alkanes are similar for samples of Rhynie Chert and shale, with the exception that the chert may have slightly high proportions of *n*-alkanes greater than C_{30} (Fig. 5). The Strathpeffer shale has notably greater proportions of isoprenoids compared to *n*-alkanes (Fig. 5). This has typically been explained as a consequence of some of the continental Devonian muddy lithologies being deposited in hypersaline lakes in which a significant proportion of the primary productivity was in the form of halophilic archaea whose cell membranes comprised tetra-ether lipids and phytol (Duncan and Hamilton, 1988; Killops and Killops, 2005).

Fewer/shorter n-alkanes occur in Devonian plant matter, which may have lacked waxy leaves (Song et al., 2017; Blumenberg et al., 2018, but see Martinez et al., 2019). The paucity of n-alkanes above C_{25} should not, therefore, be interpreted to indicate a lack of higher plants. However, the *m/z* 85 chromatograms for grey shales (Fig. 5) suggest that the contribution from higher plants may be lower than in the cherts, and the organic matter was rather dominated by algae/bacteria/cyanobacteria.

In addition to differences between the proportions of *n*-alkanes and isoprenoids, samples of the Rhynie Chert mostly have higher ratios of pristane/phytane (Pr/Ph) and C_{29} 17α,21β(H) hopane to C_{30} 17α,21β(H) hopane, than the Strathpeffer shales (Fig. 8 a,b). These ratios compare the relative abundance of homologous compounds where the numerator is a lower carbon number (pristane and C_{29} hopane), that can form by oxidising of a higher carbon precursor (Hughes et al., 1995; Peters et al., 2005). Anoxic conditions in the depositional environment restrict oxidising reactions and preserve higher carbon number homologues, thus on the basis of these biomarker proxies it might be concluded that sedimentary organic matter in the Rhynie chert experienced more persistently oxic conditions than the sedimentary organic matter in the

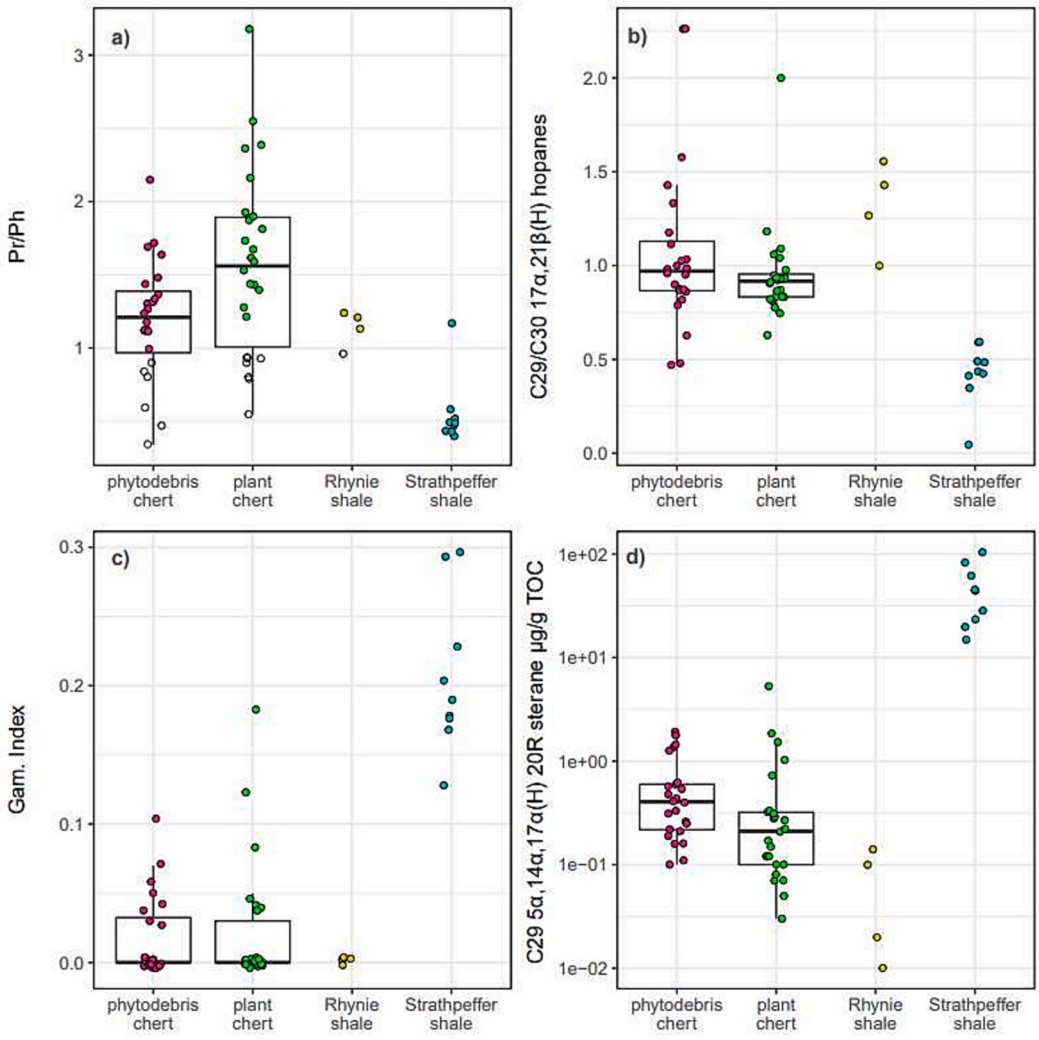

Fig. 8. Quantitative data for biomarkers in Rhynie Chert, and shales at Rhynie and Strathpeffer. (a) Pristane/Phytane (Pr/Ph) ratio; (b) C_{29}/C_{30} hopanes; (c) gammacerane index; (d) C_{29} steranes/TOC.

shales. Qualitatively, Pr/Ph values in the range 1 to 3 could be interpreted to result from dysoxic conditions, similar to that experienced by deltaic sediments where sedimentary organic matter is at least periodically subaerially exposed (Hughes et al., 1995). However, although likely uncommon in typical sedimentary settings, pristane can also derive from side chain cleavage of tocopherols (Goossens et al., 1984; Maeda et al., 2006) a group of compounds found in plants. Samples of Rhynie Chert with intact plant fragments have the highest ratios of pristane to phytane (Fig. 8a), thus the higher proportion of pristane in these samples may reflect production by vascular plants as well as the subaerial nature of the hydrothermal spring.

5.2.2. *Higher plants*

Aromatic compounds cadalene and retene were detected in numerous samples. Cadalene was recorded in almost all Rhynie Chert samples and also the Rhynie shale samples, and some of the Strathpeffer samples. Retene also occurs in several, but many fewer, Rhynie Chert samples. The biomarkers cadalene and retene are ubiquitous signatures of higher plants. Cadalene is taken as an indication of higher plant contribution to organic matter, back to the Middle Devonian (Philp and De Garmo, 2020), and retene in Palaeozoic rocks is probably derived from compounds with a kaurane-type skeleton in pre-vascular plants and algae (Romero-Sarmiento et al., 2010). The uniformly low retene/cadalene ratios (mostly <0.1) in Rhynie samples are typical of a pre-conifer plant assemblage recorded in younger rocks (Hautevelle et al., 2006).

Diterpenoids were identified in samples of the Rhynie Chert, including C_{18}-C_{20} tricyclic terpanes, *ent*-beyerane, kaurane, and phyllocladane (Fig. 6). The distribution of diterpenoids varies through the sample set (Fig. 10), and defines three stages. In terms of the plant assemblages (observations of Powell et al., 2000 Trewin and Fayers, 2015), samples dominated by the vascular plants *Rhynia* (trench; blocks 4 and 5, borehole 19C) and *Asteroxylon* (trench beds 1 and 2) all contain *ent*-beyerane and *ent*-kaurane. The occurrence of *ent*-beyerane in the cherts which contain *Rhynia* and *Asteroxylon* is consistent with earlier suggestions that *ent*-beyerane is synthesized in vascular plants (Romero-Sarmiento et al., 2011; Song et al., 2017). A larger set of samples, including cherts rich in the plants *Horneophyton* and *Nothia* (trench beds 3, 5 and 14) contain *ent*-kaurane, but not *ent*-beyerane. Ancient *ent*-kaurane is attributed to synthesis in pre-vascular plants (Romero-Sarmiento et al., 2010, 2011), and modern liverworts are a source of the compound and its derivatives (Qu et al., 2008). While the kaurane skeleton was developed in compounds in the pre-vascular plants, the beyerene skeleton may have been lacking. *Ent*-beyerane is a diagenetic degradation product of *ent*-beyerol, the parent hydrocarbon of a tetracyclic diterpene found in higher plants (Noble et al., 1985). Most samples from the upper part of the section (trench beds 8 and 9, borehole 19C) have not yielded diterpenoids.

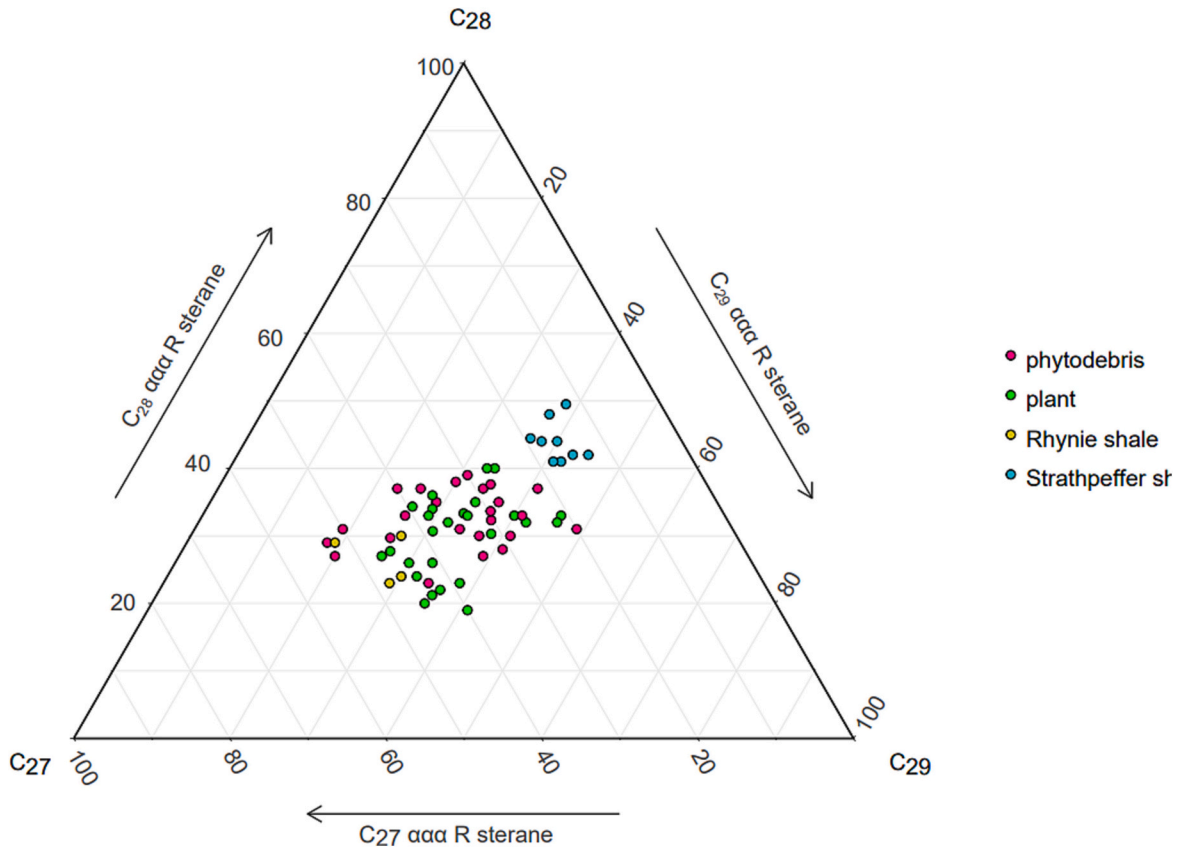

Fig. 9. Ternary plot of C_{27}, C_{28} and C_{29} steranes in Rhynie Chert, and shales at Rhynie and Strathpeffer.

Hitherto, the earliest records of *ent*-beyerane were in Middle Devonian coals from China (Song et al., 2017). Younger occurrences of *ent*-beyerane have been reported in a few coals of Lower Carboniferous age (Romero-Sarmiento et al., 2011; Blumenberg et al., 2018), and then are common from the Upper Carboniferous onwards.

Diterpenoids are important in plant-fungus symbiosis. By analogy with the function of modern terpene derivatives, diterpenoid synthesis in the Devonian was likely a defence against diseases and pests, including fungal pathogens (Karunanithi and Zerbe, 2019). Terpenoids in vascular plants also deter predation by herbivorous insects and other arthropods (Mumm et al., 2008; Sharma et al., 2017). Fungi and arthropods are so widespread in the Rhynie Chert (Trewin and Kerp, 2017) that diterpenoid synthesis was a likely response to protect the plants. Nevertheless, genes involved in diterpene synthesis in plants were in turn acquired by fungi and became involved in fungal metabolism (Fischer et al., 2015). This included a positive feedback role for fungal diterpenes as hormones in plant-fungus symbiosis (Schardl et al., 2013).

5.2.3. Steranes

A ternary diagram illustrating the proportions of 5α14α17α R steranes (Fig. 9) shows that the samples of Rhynie Chert are intermediate between the Rhynie and Strathpeffer shales. The Strathpeffer shale has a higher proportion of C_{28} sterane, a characteristic typically associated with sedimentary organic matter from lakes (Huang and Meinschein, 1979; Grantham and Wakefield, 1988), whereas the Rhynie shale has a greater proportion of C_{27} sterane, a characteristic that in other circumstances is typical of marine sedimentary organic matter. In this instance, the high proportion of C_{27} sterane in the Rhynie shale more likely represents the production of higher proportions of precursor C_{27} sterols (such as cholesterol) by zookplankton (Huang and Meinschein, 1979; Kodner et al., 2008). Thus, the relatively high-C_{27} sterane composition for the lacustrine Rhynie shales suggests a broader community, including animal life, than the plant-rich Rhynie Chert. In contrast, in the Strathpeffer hypersaline environment, C_{28} and C_{29} sterol precursors were produced by phytoplankton (Volkman, 2003).

The C_{29} sterol precursors can derive from both plant sterols, as well as sterols synthesized by algae (green algae, Volkman, 2003). Although the proportions of C_{29} and C_{28} steranes are similar for both the Rhynie Chert and Rhynie shale, the Rhynie Chert contains an order of magnitude higher absolute concentrations of C_{29} sterane than the Rhynie shale. Given the presence of fossil plants in the cherts, this feature of the sterane composition reflects a higher total amount of C_{29} sterols that can be derived from higher plants. The very high concentrations of C_{29} steranes in the Strathpeffer shale (Fig. 8d) is due to the high productivity of the environment.

5.2.4. Decomposers: fungi and bacteria

Perylene was identified in some samples (Figs. S6, S7), including samples in borehole 19C which were recorded as fungi-rich by petrography (Fig. 3) (Powell et al., 2000). Perylene has been proposed as an indicator of fungal decay of woody matter (Grice et al., 2009; Marynowski et al., 2013) in younger rocks. If the identification was extended to indicate degradation of plant matter in older rocks, its identification would be consistent with the abundance of fungi previously observed in the Rhynie Chert (Powell et al., 2000; Taylor et al., 2004; Strullu-Derrien et al., 2014; Krings et al., 2018). However, it is important to note that recent evaluation of perylene indicates the link to fungi is not at all definitive (Li et al., 2022), and the occurrence is reported here to add to the database of identifications. The occurrence at Rhynie is also in rocks at a higher maturity than the limit of about 0.7% Ro which is hitherto assumed for perylene. Perylene *is* found in moderately abundant amounts at geothermal sites in sedimentary rocks in Iceland, deposited over a similar temperature range (largely <100 °C) to the Rhynie siliceous sediments (Geptner et al., 2005, 2006). This is an analogous

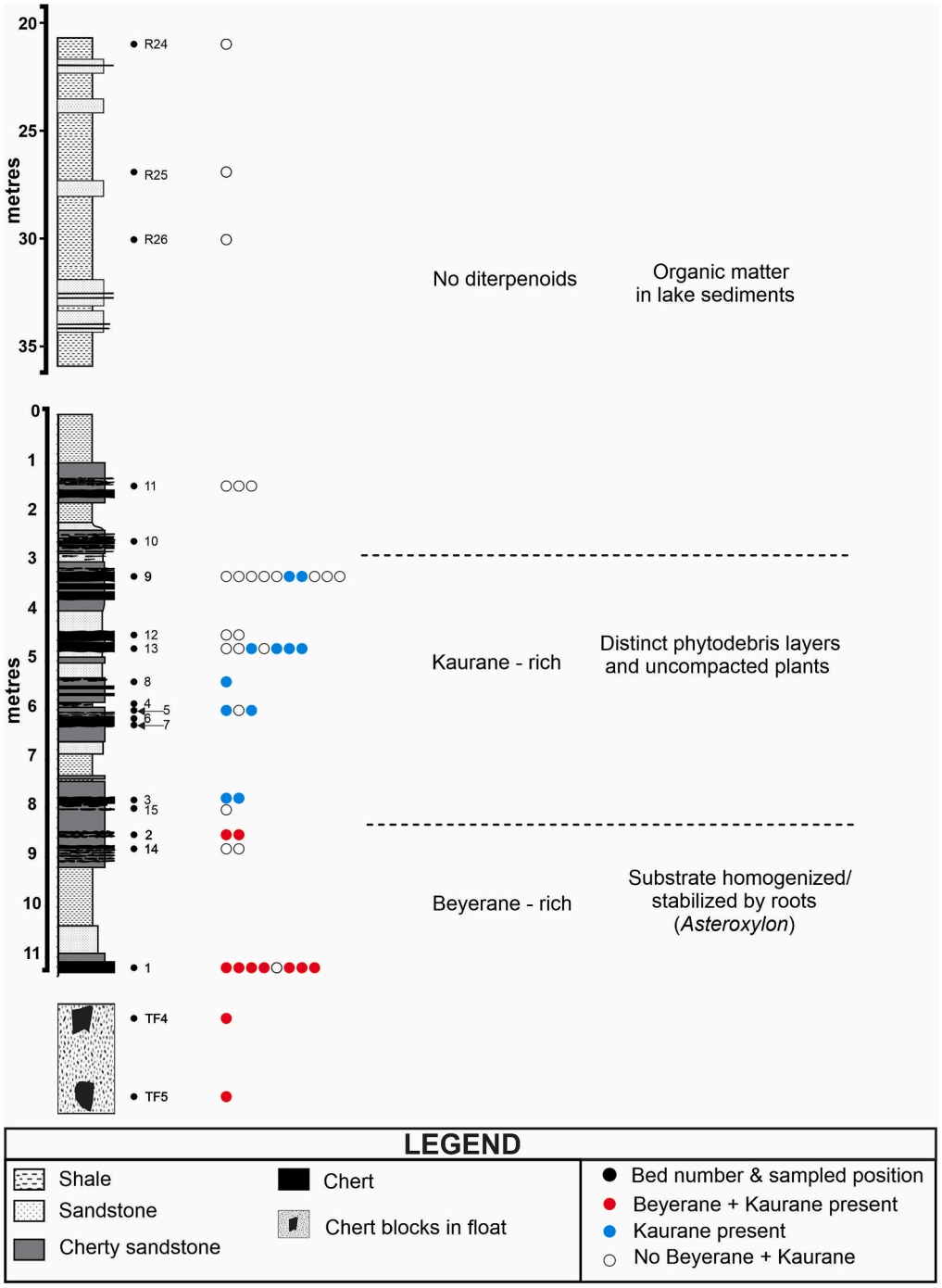

Fig. 10. Distribution of diterpenoids through Rhynie section. Most samples in lower part of combined trench 03/T1 (0 to 12 m) and borehole 19C section (21 to 36 m) contain the plant *Asteroxylon*, and the biomarkers *ent*-beyerane and *ent*-kaurane. Overlying section contains samples with the plants *Horneophyton* and *Nothia*, and just *ent*-kaurane, followed by section with no diterpenoids.

environment which may help to explain what is otherwise an anomalous occurrence of perylene. Perylene was also recorded in the carbonaceous grey shales of borehole 19C. As in other published occurrences in Devonian shales (Tulipani et al., 2015; Philp and De Garmo, 2020), the perylene is implied to be washed off a terrestrial surface. No perylene was detected in any of the 9 shale samples from Strathpeffer, or from a control sample of andesite at Rhynie, which excludes the possibility of a contribution from modern fungi.

Similarly, the C_{29} 25-norhopane was detected in many of the Rhynie Chert samples, but not in the Strathpeffer shale samples. This difference suggests that the degradation was a feature of the depositional environment, rather than alteration of lithified sediments after uplift. Most previous records of 25-norhopanes are signatures of biodegraded oils or lithified shales, but they also form where organic matter was microbially altered before burial (Cao et al., 2008). As these biomarkers are preserved within silica from hot springs, they represent degradation in the surface soil zone, rather than during subsequent burial, so the decomposers formed part of the surface biota.

5.2.5. *Gammacerane*

Many of the Rhynie Chert samples, but none of the Rhynie shale samples, contain gammacerane (Fig. 8c). All the Strathpeffer shale

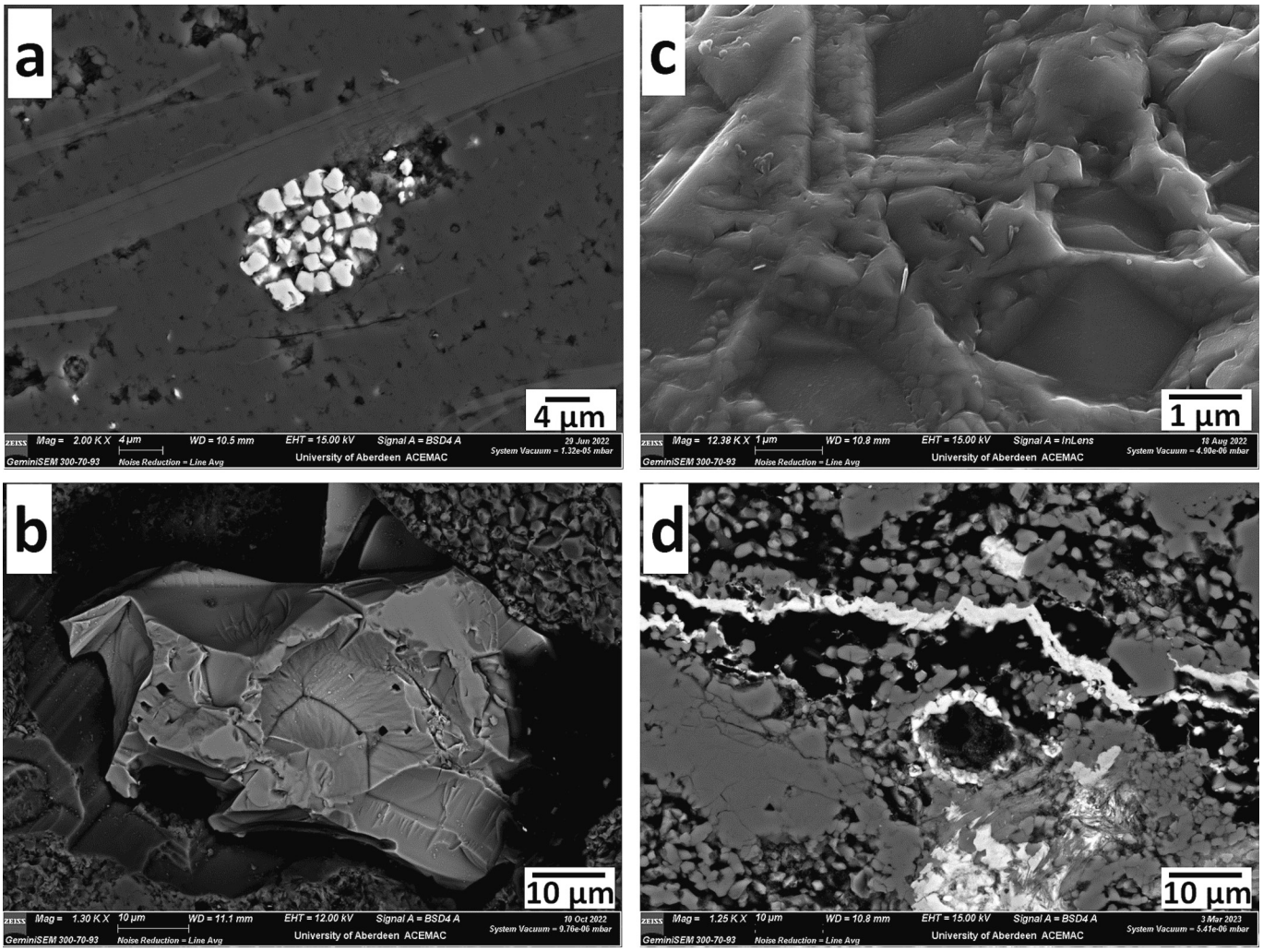

Fig. 11. Backscattered electron images showing minerals in Rhynie Chert representing biological activity. A, Pyrite framboid, typical of bacterial activity in reduced environments. B, Detrital garnet grain exhibiting sub-micron dissolution pits. C, Irregular surface of altered monazite grain, showing stubby re-growths of monazite on surface. D, Coatings of iron-rich oxides (bright) on and around detrital plant matter (black). Samples carbon-coated.

samples contain gammacerane. The mean gammacerane index, which measures the abundance relative to a bacterially-derived hopane, is much lower in Rhynie Chert (mean 0.02) than in Strathpeffer (mean 0.21). These values are low and high relative to a benchmark division of values at 0.15 (Hao et al., 2009). The high value for the Strathpeffer samples is typical of a hypersaline environment, evidenced by replaced gypsum in the shales (Parnell, 1985), and further supported by the detection of β-carotane in all of the samples. Gammacerane could conceivably indicate elevated salinity at Rhynie in waters of the hot spring system. Although gammacerane is interpreted as asalinity indicator, it is also deposited in diverse other environments, including fossil fungi (Drake et al., 2021), which would be possible at Rhynie. No β-carotane was detected in Rhynie samples.

5.3. Mineral biomarkers

Pyrite framboids are abundant in the plant-bearing cherts (Fig. 11), and they were encased by the earliest silica. The pyrite must have been precipitated almost immediately to be included in the pre-compaction silica. This implies a waterlogged, reduced environment, which is consistent with the evidence of biodegradation. Framboidal-textured pyrite is very commonly developed within decaying organic matter, including in plant debris (Garcia-Guinea et al., 1998; Grimes et al., 2002). Pyrite, at least some of which is framboidal, is found in other Lower Devonian terrestrial plant matter in Britain (Rayner, 1984; Kenrick and Edwards, 1988), and as at Rhynie occurs directly associated with organic matter and formed pre-compaction. Framboidal pyrite is probably a consequence of bacterial decay (Wacey et al., 2015). Additionally, under anaerobic conditions, sulphate-reducing bacteria may form consortia with fungal mycelia on decomposing organic matter, and precipitate pyrite (Borkow and Babcock, 2003), as at Rhynie. Higher degrees of pyritization (DOP values) are recorded in the plant beds compared to the phytodebris beds (Parnell et al., 2022).

The study encountered grains exhibiting holes (Fig. 12) that can be understood by modern analogues. Mitchell et al. (2019) described grains in modern Icelandic soils which exhibit biologically mediated weathering, including holes/tunnels, authigenic mineral precipitates (Fe-rich in this case) and fretted surfaces. Tunnelling of grains by fungi is widely observed (Hoffland et al., 2003; Smits, 2006; van Schöll et al., 2008), and the tunnels may include filamentous structures which are direct evidence of their fungal origin (Mitchell et al., 2021). The Rhynie mica grain surfaces similarly exhibit holes, mineral precipitates and fretted surfaces. The holes are of comparable size, about 2 µm in diameter, and have a comparable spatial density of about thirty 2 µm holes/µm^2. In addition, many sub-micron holes occur in both cases. Holes in modern grains show bright rims in SEM images due to heavier elements (Mitchell et al., 2021), which is replicated closely by the bright rims around holes in Rhynie grains. In both cases the rims contain sulphur. The particular

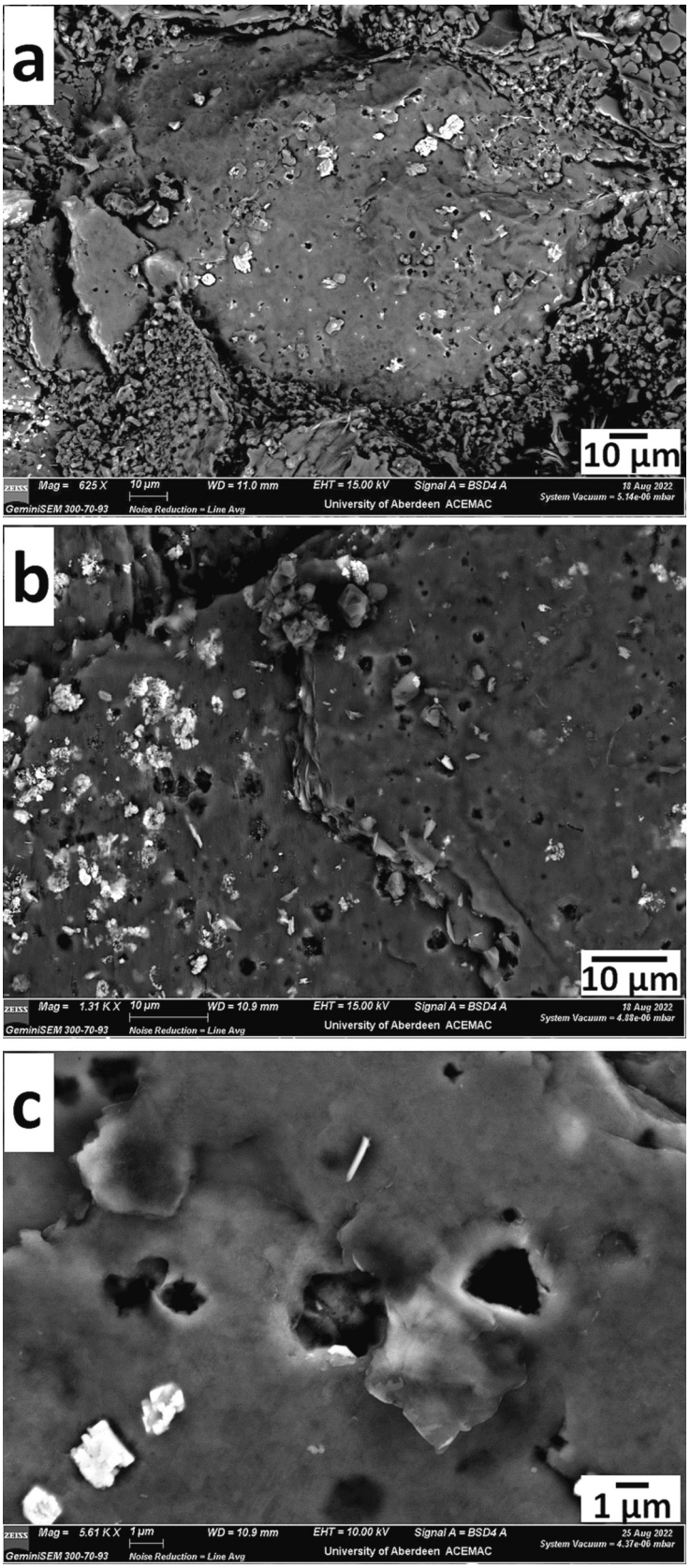

Fig. 12. Backscattered electron images showing altered detrital mica grains in Rhynie Chert, attributable to biological activity. A, Rounded detrital mica grain, exhibiting dissolution pits, and crystals of authigenic monazite (bright) on grain surface. B, Close-up of grain surface, showing pitted mica and monazite grains. C, Further close-up of dissolution pits showing bright (sulphur-rich) rims as found around modern fungal pitting. Samples carbon-coated.

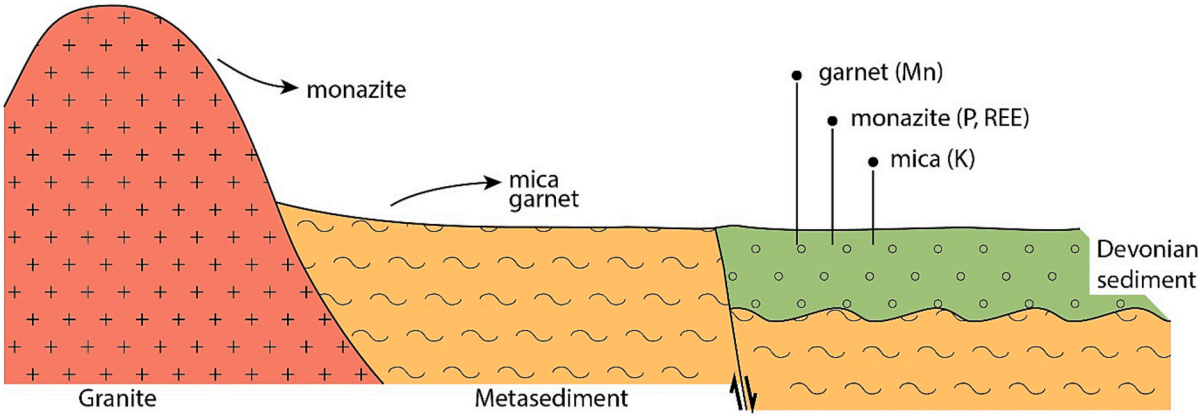

Fig. 13. Schematic summary of mineral provenance for bioavailable elements in Devonian sediment at Rhynie. Monazite from granite, and mica and garnet from metasediments, supply bioavailable P/REE, K and Mn respectively.

occurrence of holes in muscovite micas is consistent with the targeting of such grains to extract potassium by fungi (e.g., van Schöll et al., 2006; Quirk et al., 2012; Song et al., 2015). Further, the holes occur mostly in altered muscovite, which is probably phengitic, inherited from phengitic micas in the Dalradian Supergroup and Caledonian granites which were eroded to form the Devonian sediments. Holes are present in both polished and unpolished samples, which excludes polishing as a cause of hole formation.

In addition to the pitted micas, the detrital grain assemblage in the Rhynie Chert includes pitted monazite and pitted garnet (Fig. 11). Both minerals are known to be dissolved by microbiota as a strategy to release nutrients. Monazite in particular releases phosphorus, which is essential to plant-fungal symbiosis which supplies phosphorus to plants (Corbett et al., 2017; Castro et al., 2020). The dissolution of garnet by microbes would release manganese and other trace elements (Ivarsson et al., 2018).

The alteration of detrital grains and the authigenic mineralogy in the chert may be linked. The garnet grains would have released manganese when altered, and the Rhynie pyrite is unusually enriched in manganese. Coatings of manganese-iron oxides on plant debris (Parnell et al., 2022) also indicate manganese availability, and by analogy with modern soils may have been mitigated by fungi (Santelli et al., 2011). Similarly, rare earths and phosphorus released during the alteration of detrital monazite could be the source of the authigenic monazite that mineralizes altered mica grains (Fig. 12).

The authigenic mineral precipitates in Rhynie grain surfaces include titanium-iron oxides, which may be similar to the iron-rich precipitates recorded on modern grains by Mitchell et al. (2019). However, the Rhynie grains also include widespread neoformed monazite, which is exceptional in any low-temperature environment. The occurrence of monazite indicates a source of both rare earth elements (REEs) and phosphate, most probably from a very proximal source, given the local abundance required. The occurrence of REE-bearing fluorocarbonate mineralization in the shales (Parnell et al., 2023) also indicates REE mobility. The most likely source would be pre-existing monazite. The potential for localized redistribution of monazite in sedimentary rocks is shown by monazite overgrowths on detrital monazite grains in sandstone (Milodowski and Zalasiewicz, 1991; Allaz et al., 2013). Monazite overgrowths are a consequence of low-temperature non-biological processes, but there is also evidence in previous studies for phosphate mineralization by fungi and bacteria, including monazite neoformation (Taunton et al., 2000; Cheng et al., 2018).

It is difficult to prove unequivocally that the molecular and mineral biomarkers are directly coupled, i.e., the molecular evidence of fungi and bacterial decomposition is related to the observed mineral diagenesis. However, a relationship is suggested by:

(i) The molecular and mineral data is derived from the same limited suite of samples collected within an area of <100 m^2.
(ii) The organic matter and minerals were both sealed at a very early stage by hot spring silicification, so the data reflect a very limited time window.
(iii) There is no alternative explanation for the observed mineral features.
(iv) The plant beds and phytodebris beds show distinctions in both the molecular (Pr/Ph) and mineral (DOP) data.

6. Conclusions

The data show that it is possible to obtain good quality signatures for a wide range of organic biomarkers in the Rhynie Chert. Specific biomarkers for several of the main components of the ecosystem can be identified readily. The components include higher plants (cadalene, diterpenoids), fungi (perylene??) and biodegradation (25-norhopanes). Each of these characteristic biomarkers is present in at least 45% of the Rhynie Chert samples. Lacustrine shales in the Rhynie Chert succession show distinctive compositions, characterized by the lack of the C_{29} 25-norhopane and gammacerane. The Lower Devonian rocks of Strathpeffer are also distinct, characterized by lack of perylene, and abundant gammacerane. The environment at Strathpeffer was different to that at Rhynie, characterized by hypersalinity, high productivity and lack of any evidence of decomposition. These distinctions emphasize the fidelity of the data.

The new data help to understand the hot spring environment, which is important as a residence for diverse life, including during terrestrialization, and as a source of novel microbial life with potential for technological advances (Sen et al., 2014; Jardine et al., 2018).

The mineral component of the ecosystem shows evidence for a biological contribution to authigenesis and alteration. Pyrite framboids, heavily leached monazite and garnet, and dissolution pits in micas comparable with pits formed by modern fungi, may all be regarded as mineralogical biomarkers. The geological landscape at Rhynie made several important elements bioavailable as detrital grains. Monazite from granite, and mica and garnet from metasediments, supplied phosphorus, potassium and manganese respectively (Fig. 13). Each of these elements can be liberated by fungi.

The data from Rhynie, supported by data from Strathpeffer, show that the earliest terrestrial ecosystem is recorded by an assemblage of molecular and mineral biomarkers. Together with the physical fossil record (Edwards et al., 2018; Strullu-Derrien et al., 2019) and phylogenetic analysis (Gerrienne et al., 2016; van Straalen, 2021; Tihelka et al., 2022), the investigation of terrestrialization is open to a multifaceted approach.

CRediT authorship contribution statement

T.O. Akinsanpe: Writing – review & editing, Validation, Supervision, Methodology, Investigation. **S.A. Bowden**: Writing – review & editing, Supervision. **J. Parnell:** Writing – original draft, Supervision, Project administration, Investigation, Funding acquisition, Conceptualization.

Declaration of competing interest

The authors declare that they have no known competing financial interests or personal relationships that could have appeared to influence the work reported in this paper.

Data availability

Data is supplied as Supplementary Material

Acknowledgement

The study depended on material archived by N.H. Trewin, C.M. Rice, S. Fayers and L.I. Anderson. We acknowledge C. Taylor, J. Still, J. Johnston, W. Ritchie and J. Bowie for skilled technical support. A. Schito kindly performed the Raman spectroscopy. We are very grateful to Professor Armelle Riboulleau, Universite de Lille, who provided a sample of SKT-D. The study was partly supported by the Natural Environment Research Council (grant NE/T003677/1). We are grateful for the comments of anonymous reviewers which greatly improved the manuscript.

Appendix A. Supplementary data

Supplementary data to this article can be found online at https://doi.org/10.1016/j.palaeo.2024.112101.

References

Abbott, G.D., Fletcher, I.W., Tardio, S., Hackz, E., 2017. Exploring the geochemical distribution of organic carbon in early land plants: a novel approach. Philos. Trans. R. Soc. B 373, 20160499.
Allaz, J., Selleck, B., Williams, M.L., Jercinovic, M.J., 2013. Microprobe analysis and dating of monazite from the Potsdam Formation, New York: a progressive record of chemical reaction and fluid interaction. Am. Mineral. 98, 1106–1119.
Aoki, K., Windley, B., Sato, K., Sawaki, Y., Kawai, T., Shibuya, T., Kumagai, H., Suzuki, K., Maruyama, S., 2013. Chemical composition and K–Ar age of Phengite from Barrovian metapelites, Loch Leven, Scotland. J. Geol. Soc. Jpn. 119, 437–442.
Baron, M., Hillier, S., Rice, C.M., Czapnik, K., Parnell, J., 2004. Fluids and hydrothermal alteration assemblages in a Devonian gold-bearing hot-spring system, Rhynie, Scotland. Trans. R. Soc. Edinb. Earth Sci. 94, 309–324.
Blumenberg, M., Weniger, P., Kus, J., Scheeder, G., Piepjohn, K., Zindler, M., Reinhardt, L., 2018. Geochemistry of a middle Devonian cannel coal (Munindalen) in comparison with Carboniferous coals from Svalbard. Arktos 4, 1–8.
Böcker, J., Littke, R., Hartkopf-Froder, C., Jasper, K., Schwarzbauer, J., 2013. Organic geochemistry of Duckmantian (Pennsylvanian) coals from the Ruhr Basin, western Germany. Int. J. Coal Geol. 107, 112–126.
Borkow, P.S., Babcock, L.E., 2003. Turning pyrite concretions outside-in: Role of biofilms in pyritization of fossils. Sediment. Record 1, 4–7.
Cao, J., Hu, K., Wang, K., Bian, L., Liu, Y., Yang, S., Wang, L., Chen, Y., 2008. Possible origin of 25-norhopanes in Jurassic organic-poor mudstones from the northern Qaidam Basin (NW China). Org. Geochem. 39, 1058–1065.
Cascales-Miñana, B., Steemans, P., Servais, T., Lepot, K., Gerrienne, P., 2019. An alternative model for the earliest evolution of vascular plants. Lethaia 52, 445–453.
Castro, L., Blázquez, M.L., González, F., Muñoz, J.A., 2020. Bioleaching of phosphate minerals using Aspergillus Niger: Recovery of copper and rare earth elements. Metals 10, 978.
Cheng, Y., Zhang, L., Bian, X., Zuo, H., Dong, H., 2018. Adsorption and mineralization of REE-lanthanum onto bacterial cell surface. Environ. Sci. Pollut. Res. 25, 22334–22339.
Clarke, P., Parnell, J., 1999. Facies analysis of a back-tilted lacustrine basin in a strike-slip zone, lower Devonian, Scotland. Palaeogeogr. Palaeoclimatol. Palaeoecol. 151, 167–190.
Cook, J.W., Hewett, C.L., Hieger, I., 1933. The isolation of a cancer-producing hydrocarbon from coal tar. J. Chem. Soc. 106, 395–405.
Corbett, M.K., Eksteen, J.J., Niu, X.-Z., Croue, J.-P., Watkin, E.L., 2017. Interactions of phosphate solubilising microorganisms with natural rare-earth phosphate minerals: a study utilizing Western Australian monazite. Bioprocess. Bio-syst. Eng. 40, 929–942.
Dempster, T.J., 1992. Zoning and recrystallization of phengitic micas: implications for metamorphic equilibration. Contrib. Mineral. Petrol. 109, 526–537.
Drake, H., Ivarsson, M., Heim, C., Snoeyenbos-West, O., Bengston, S., Belivanova, V., Whitehouse, M., 2021. Fossilized anaerobic and possibly methanogenesis-fueling fungi identified deep within the Siljan impact structure, Sweden. Communicat. Earth Environ. 2, 34.
Duncan, A.D., Hamilton, R.F.M., 1988. Palaeolimnology and organic geochemistry of the Middle Devonian in the Orcadian Basin. In: Fleet, A.J., Kelts, K., Talbot, M.R. (Eds.), Lacustrine Petroleum Source Rocks. Geological Society, vol. 40. Special Publications, London, pp. 173–201.
Dzou, L.I.P., Noble, R.A., Senftle, J.T., 1995. Maturation effects on absolute biomarker concentrations in a suite of coals and associated vitrinite concentrates. Org. Geochem. 23, 681–697.
Edwards, D., Kenrick, P., Dolan, L., 2018. History and contemporary significance of the Rhynie cherts—our earliest preserved terrestrial ecosystem. Philos. Trans. R. Soc. Lond. B 373, 20160489.
Escuder-Rodríguez, J.-J., DeCastro, M.-E., Saavedra-Bouza, A., Becerra, M., González-Siso, M.-I., 2022. Insights on microbial communities inhabiting non-volcanic hot springs. Int. J. Mol. Sci. 23, 12241. https://doi.org/10.3390/ijms232012241.
Fang, R., Li, M., Wang, T.-G., Zhang, L., Shi, S., 2015. Identification and distribution of pyrene, methylpyrenes and their isomers in rock extracts and crude oils. Org. Geochem. 83–84, 65–76.
Fayers, S.R., Trewin, N.H., 2004. A review of the palaeoenvironments and biota of the Windyfield chert. Trans. R. Soc. Edinb. Earth Sci. 94, 325–339.
Fischer, M.J., Rustenhloz, C., Leh-Louis, V., Perrière, P., 2015. Molecular and functional evolution of the fungal diterpene synthase genes. BMC Microbiol. 15, 221.
Fox, F., 1889. Strathpeffer Spa, its Climate and Waters. With Observations Historical, Medical, and General, Descriptive of the Vicinity, Etc. H.K. Lewis, London, p. 165.
Garcia-Guinea, J., Martinez-Frías, J., Harffy, M., 1998. Cell-hosted pyrite framboids in fossil woods. Naturwissenschaften 85, 78–81.
Geptner, A., Kristmannsdottir, H., Yurii Pikovskii, Y., Richter, B., 2005. Abiogenic hydrocarbon's emission in the modern rift zone, Iceland. In: Proceedings, World Geothermal Congress, Antalya, Turkey, 24–29 April 2005, pp. 1–7.
Geptner, A.R., Richter, B., Pikovskii, Y.I., Chernyansky, S.S., Alekseeva, T.A., 2006. Hydrothermal polycyclic aromatic hydrocarbons in marine and lagoon sediments at the intersection between Tjörnes Fracture Zone and recent rift zone (Skjálfandi and Öxarfjörður bays), Iceland. Mar. Chem. 101, 153–165.
Gerrienne, P., Servais, T., Vecoli, M., 2016. Plant evolution and terrestrialization during Palaeozoic times—the phylogenetic context. Rev. Palaeobot. Palynol. 227, 4–18.
Gomez, F., 2011. Hot Spring Microbiology. In: Gargaud, M. (Ed.), Encyclopedia of Astrobiology. Springer, Berlin, Heidelberg. https://doi.org/10.1007/978-3-642-11274-4_74.
Goossens, H., de Leeuw, J., Schenck, P., et al., 1984. Tocopherols as likely precursors of pristane in ancient sediments and crude oils. Nature 312, 440–442. https://doi.org/10.1038/312440a0.
Grantham, P.J., Wakefield, L.L., 1988. Variations in the sterane carbon number distributions of marine source rock derived crude oils through geological time. Org. Geochem. 12, 61–73.
Grice, K., Hong, L., Atahan, P., Asif, M., Hallmann, C., Greenwood, P., Maslen, E., Tulipani, S., Williford, K., Dodson, J., 2009. New insights into the origin of perylene in geological samples. Geochim. Cosmochim. Acta 73, 6531–6543.
Grimes, S.T., Davies, K.L., Butler, I.B., Fiona Brock, F., Edwards, D., Rickard, D., Briggs, D.E.G., Parkes, R.J., 2002. Fossil plants from the Eocene London Clay: the use of pyrite textures to determine the mechanism of pyritization. J. Geol. Soc. Lond. 159, 493–501.
Hao, F., Zhou, X., Zhu, Y., Bao, X., Yuanyuan, Y., 2009. Charging of the Neogene Penglai 19-3 field, Bohai Bay Basin, China: Oil accumulation in a young trap in an active fault zone. AAPG Bull. 93, 155–179.
Harrison, T.N., 1990. Chemical variation in micas from the Cairngorm pluton, Scotland. Mineral. Mag. 54, 355–366.
Hautevelle, Y., Michels, R., Malartre, F., Trouiller, A., 2006. Vascular plant biomarkers as proxies for palaeoflora and palaeoclimatic changes at the Dogger/Malm transition of the Paris Basin (France). Org. Geochem. 37, 610–625.
Hoffland, E., Giesler, R., Jongmans, A.G., van Breemen, N., 2003. Feldspar tunneling by fungi along natural productivity gradients. Ecosystems 6, 739–746.
Huang, W.Y., Meinschein, W.G., 1979. Sterols as ecological indicators. Geochim. Cosmochim. Acta 43, 739–745.
Hughes, W.B., Holba, A.G., Dzou, L.I.P., 1995. The ratios of dibenzothiophene to phenanthrene and pristane to phytane as indicators of depositional environment and lithology of petroleum source rocks. Geochim. Cosmochim. Acta 59, 3581–3598.
Ivarsson, M., Skogby, H., Phichaikamjornwut, B., Bengtson, S., Siljeström, S., Ounchanum, P., Boonsoong, A., Kruachanta, M., Marone, F., Belivanova, V., Holmström, S., 2018. Intricate tunnels in garnets from soils and river sediments in Thailand - possible endolithic microborings. PLoS One 18, e0200351. https://doi.org/10.1371/journal.pone.0200351.
Jardine, J.L., Stoychev, S., Mavumengwana, V., Ubomba-Jaswa, E., 2018. Screening of potential bioremediation enzymes from hot spring bacteria using conventional plate assays and liquid chromatography - Tandem mass spectrometry (Lc-Ms/Ms). J. Environ. Manag. 223, 787–796.
Kang, X., Csetenyi, L., Gadd, G.M., 2021. Colonization and bioweathering of monazite by Aspergillus Niger: solubilization and precipitation of rare earth elements. Environ. Microbiol. 23, 3970–3986.
Karunanithi, P.S., Zerbe, P., 2019. Terpene synthases as metabolic gatekeepers in the evolution of plant terpenoid chemical diversity. Front. Plant Sci. 10, 1166.

Kenrick, P., Edwards, D., 1988. The anatomy of lower Devonian *Gosslingia breconensis* heard based on pyritized axes, with some comments on the permineralization process. Bot. J. Linn. Soc. 97, 95–123.
Killops, S.D., Killops, V.J., 2005. Introduction to Organic Geochemistry, Second edition. Blackwell Publishing, Oxford.
Kodner, R.B., Pearson, A., Summons, R.E., Knoll, A.H., 2008. Sterols in red and green algae: quantification, phylogeny, and relevance for the interpretation of geologic steranes. Geobiology 6, 411–420.
Krings, M., Harper, C.J., Taylor, E.L., 2018. Fungi and fungal interactions in the Rhynie chert: a review of the evidence, with the description of Perexiflasca tayloriana gen. Et sp. nov. Philos. Trans. R. Soc. B 373, 20160500.
Li, Z., Huang, H., Yan, G., Xu, Y., George, S.C., 2022. Occurrence and origin of perylene in Paleogene sediments from the Tasmanian Gateway, Australia. Org. Geochem. 168, 104406.
Lian, B., Wang, B., Pan, M., Liu, C.Q., Teng, H.H., 2008. Microbial release of potassium from K-bearing minerals by thermophilic fungus Aspergillus fumigatus. Geochim. Cosmochim. Acta 72, 87–98.
Loron, C.C., Dzul, E.R., Orr, P.J., Gromov, A.V., Fraser, N.C., McMahon, S., 2023. Molecular fingerprints resolve affinities of Rhynie chert organic fossils. Nat. Commun. 14, 1387.
Lutzoni, F., et al., 2018. Contemporaneous radiations of fungi and plants linked to symbiosis. Nat. Commun. 9, 5451.
Maeda, H., Song, W., Sage, T.L., Della, Penna D., 2006. Tocopherols play a crucial role in low-temperature adaptation and phloem loading in Arabidopsis. Plant Cell 18, 2710–2732.
Manson, D., 1879. On the Sulphur Waters of Strathpeffer, in the Highlands of Ross-Shire, with District Guide. J. & A. Churchill, London.
Martinez, A., Boyer, D.L., Droser, M.L., Barrie, C., Love, G.D., 2019. A stable and productive marine microbial community was sustained through the end-Devonian Hangenberg Crisis within the Cleveland Shale of the Appalachian Basin, United States. Geobiology 17, 27–42.
Marynowski, L., Smolarek, J., Bechtel, A., Phillippe, M., Kurkiewicz, S., Simoneit, B.R.T., 2013. Perylene as an indicator of conifer fossil wood degradation by wood-degrading fungi. Org. Geochem. 59, 143–151.
Milodowski, A.E., Zalasiewicz, J.A., 1991. Redistribution of rare earth elements during diagenesis of turbidite/hemipelagite mudrock sequences of Llandovery age from Central Wales. Geol. Soc. Lond. Spec. Publ. 57, 101–124. https://doi.org/10.1144/GSL.SP.1991.057.01.10.
Mitchell, R.L., Strullu-Derrien, C., Kenrick, P., 2019. Biologically mediated weathering in modern cryptogamic ground covers and the early Paleozoic fossil record. J. Geol. Soc. 176, 430–439.
Mitchell, R.L., Davies, P., Kenrick, P., Volkenandt, T., Pleydell-Pearce, C., Johnston, R., 2021. Correlative microscopy: a tool for understanding soil weathering in modern analogues of early terrestrial biospheres. Sci. Rep. 11, 12736.
Mumm, R., Posthumus, M.A., Dicke, M., 2008. Significance of terpenoids in induced indirect plant defence against herbivorous arthropods. Plant Cell Environ. 31, 575–585.
Noble, R.A., Alexander, R., Kagi, R.I., Knox, J., 1985. Tetracyclic diterpenoid hydrocarbons in some Australian coals, sediments and crude oils. Geochim. Cosmochim. Acta 49, 2141–2147.
Parnell, J., 1985. Evidence for evaporites in the ORS of northern Scotland: replaced gypsum horizons in Easter Ross. Scott. J. Geol. 21, 377–380.
Parnell, J., Baba, M., Bowden, S., 2016. Emplacement and biodegradation of oil in fractured basement: the 'coal' deposit in Moinian gneiss at Castle Leod, Ross-shire. Earth Environ. Sci. Trans. R. Soc. Edinb. 107, 23–32.
Parnell, J., Akinsanpe, T.O., Armstrong, J.G.T., Boyce, A.J., Still, J.W., Bowden, S.A., Clases, D., de Vega, R.G., Feldmann, J., 2022. Trace element geochemistry in the earliest terrestrial ecosystem, the Rhynie Chert. Geochem. Geophys. Geosyst. 23 e2022GC010647.
Parnell, J., Akinsanpe, T.O., Still, J.W., Schito, A., Bowden, S.A., Muirhead, D.K., Armstrong, J.G.T., 2023. Low-temperature fluorocarbonate mineralization in lower Devonian Rhynie Chert. UK. Minerals 13, 595.
Peters, K.E., Walters, C.C., Moldowan, J.M., 2005. The Biomarker Guide. Biomarkers and Isotopes in Petroleum Exploration and Earth History. Cambridge University Press, Cambridge.
Philp, R.P., De Garmo, D., 2020. Geochemical characterization of the Devonian-Mississippian Woodford Shale from the McAlister Cemetery Quarry, Criner Hills Uplift, Ardmore Basin, Oklahoma. Mar. Pet. Geol. 112, 104078.
Powell, C.L., Trewin, N.H., Edwards, D., 2000. Palaeoecology and plant succession in a borehole through the Rhynie cherts, lower Old Red Sandstone, Scotland. In: Friend, P.F., Williams, B.P.J. (Eds.), New Perspectives on the Old Red Sandstone, Geological Society, vol. 180. Special Publications, London, pp. 439–457.
Qu, J.-B., Zhu, R.-L., Zhang, Y.-L., Guo, H.-F., Wang, X.-N., Xie, C.-F., Yu, W.-T., Ji, M., Lou, H.-X., 2008. *Ent*-Kaurane diterpenoids from the liverwort Jungermannia atrobrunnea. J. Nat. Prod. 71, 1418–1422.
Quirk, J., Beerling, D.J., Banwart, S.A., Kakonyi, G., Romero-Gonzalez, M.E., Leake, J.R., 2012. Evolution of trees and mycorrhizal fungi intensifies silicate mineral weathering. Biol. Lett. 8, 1006–1011.
Rabinowitz, H.S., Polissar, P.J., Savage, H.M., 2017. Reaction kinetics of alkenone and n-alkane thermal alteration at seismic timescales. Geochem. Geophys. Geosyst. 18, 53–69.
Rayner, R.J., 1984. New finds of *Drepanophycus spinaeformis* Göppert from the lower Devonian of Scotland. Trans. R. Soc. Edinb. Earth Sci. 75, 353–363.
Rice, C.M., Ashcroft, W.A., 2004. The geology of the northern half of the Rhynie Basin, Aberdeenshire, Scotland. Trans. R. Soc. Edinb. Earth Sci. 94, 299–308.
Rice, C.M., Ashcroft, W.A., Batten, D.J., Boyce, A.J., Caulfield, J.B.D., Fallick, A.E., Hole, M.J., Jones, E., Pearson, M.J., Rogers, G., Saxton, J.M., Stuart, F.M., Trewin, N. H., Turner, G.A., 1995. Devonian auriferous hot spring system, Rhynie, Scotland. J. Geol. Soc. Lond. 152, 229–250.
Rice, C.M., Trewin, N.H., Anderson, L.I., 2002. Geological setting of the early Devonian Rhynie cherts, Aberdeenshire, Scotland: an early terrestrial hot spring system. J. Geol. Soc. Lond. 159, 203–214.
Richardson, J.B., Rasul, S.M., 1978. Palynological evidence for the age and provenance of the lower Old Red Sandstone from the Apley Barn borehole, Witney, Oxfordshire (southern England). Proc. Geol. Assoc. 90, 27–42.
Romero-Sarmiento, M., Riboulleau, A., Vecoli, M., Versteegh, G.J.M., 2010. Occurrence of retene in upper Silurian–lower Devonian sediments from North Africa: Origin and implications. Org. Geochem. 41, 302–306.
Romero-Sarmiento, M., Riboulleau, A., Vecoli, M., Laggoun-Défarge, F., Versteegh, G.J. M., 2011. Aliphatic and aromatic biomarkers from Carboniferous coal deposits at Dunbar (East Lothian, Scotland): Palaeobotanical and palaeoenvironmental significance. Palaeogeogr. Palaeoclimatol. Palaeoecol. 309, 309–326.
Santelli, C.M., Webb, S.M., Dohnalkova, A.C., Hansel, C.M., 2011. Diversity of Mn oxides produced by Mn(II)- oxidizing fungi. Geochim. et Cosmochim. 75, 2762–2776.
Savage, H.M., Rabinowitz, H.S., Spagnuolo, E., Aretusini, S., Polissar, P.J., Di Toro, G., 2018. Biomarker thermal maturity experiments at earthquake slip rates. Earth Planet. Sci. Lett. 502, 253–261.
Schardl, C.L., Young, C.A., Hesse, U., Amyotte, S.G., Andreeva, K., Calie, P.J., et al., 2013. Plant-symbiotic fungi as chemical engineers: Multi-genome analysis of the Clavicipitaceae reveals dynamics of alkaloid Loci. PLoS Genet. 9, e1003323.
Schito, A., Corrado, S., 2020. An automatic approach for characterization of the thermal maturity of dispersed organic matter Raman spectra at low diagenetic stages. Geol. Soc. Lond. Spec. Publ. 484, 107–119.
Sedlakova-Kadukova, J., Marcincakova, R., Luptakova, A., Vojtko, M., Fujda, M., Pristas, P., 2020. Comparison of three different bioleaching systems for Li recovery from lepidolite. Sci. Rep. 10, 14594.
Sen, S.K., Raut, S., Dora, T.K., Mohapatra, P.K.D., 2014. Contribution of hot spring bacterial consortium in cadmium and lead bioremediation through quadratic programming model. J. Hazard. Mater. 265, 47–60.
Sharma, E., Anand, G., Kapoor, R., 2017. Terpenoids in plant and arbuscular mycorrhiza-reinforced defence against herbivorous insects. Ann. Bot. 119, 791–801.
Smits, M., 2006. Mineral tunnelling by fungi. In: Gadd, G.M. (Ed.), Fungi in Biogeochemical Cycles. Cambridge University Press, Cambridge.
Song, M., Pedruzzi, I., Peng, Y., Li, P., Liu, J., Yu, J., 2015. K-extraction from muscovite by the isolated fungi. Microbiol. J. 32, 771–779.
Song, D., Simoneit, B.R.T., He, D., 2017. Abundant tetracyclic terpenoids in a Middle Devonian foliated cuticular liptobiolite coal from northwestern China. Org. Geochem. 107, 9–20.
Strullu-Derrien, C., Kenrick, P., Pressel, S., Duckett, J.G., Rioult, J.-P., Strullu, D.-G., 2014. Fungal associations in Horneophyton ligneri from the Rhynie Chert (c. 407 million year old) closely resemble those in extant lower land plants: novel insights into ancestral plant–fungus symbioses. New Phytol. 203, 964–979.
Strullu-Derrien, C., Kenrick, P., Knoll, A.H., 2019. The Rhy,nie Chert. Curr. Biol. 29, R1218–R1223.
Strullu-Derrien, C., Le Hérissé, A., Goral, T., Spencer, A.R.T., Kenrick, P., 2021. The overlooked aquatic green algal component of early terrestrial environments: *Triskelia scotlandica* gen. Et sp. nov. from the Rhynie cherts. Paper. Palaeontol. 7, 709–719.
Strullu-Derrien, C., Fercoq, F., Gèze, M., Kenrick, P., Martos, F., Selosse, M.-A., Benzerara, K., Knoll, A.H., 2023. Hapalosiphonacean cyanobacteria (Nostocales) thrived amid emerging embryophytes in an early Devonian (407-million-year-old) landscape. iScience 26 (8), 107338.
Taunton, A.E., Welch, S.A., Banfield, J.F., 2000. Microbial controls on phosphate and lanthanide distributions during granite weathering and soil formation. Chem. Geol. 169, 371–382.
Taylor, T.N., Klavins, S.D., Krings, M., Taylor, E.L., Kerp, H., Hass, H., 2004. Fungi from the Rhynie Chert: a view from the dark side. Trans. R. Soc. Edinb. Earth Sci. 94, 457–473.
Tihelka, E., Howard, R.J., Cai, C., Lozano-Fernandez, J., 2022. Was there a Cambrian Explosion on land? The case of arthropod terrestrialization. Biology 11, 1516. https://doi.org/10.3390/biology11101516.
Trewin, N.H., 1994. Depositional environment and preservation of biota in the lower Devonian hot-springs of Rhynie, Aberdeenshire, Scotland. Trans. R. Soc. Edinb. Earth Sci. 84, 433–442.
Trewin, N.H., Fayers, S.R., 2015. Macro to micro aspects of the plant preservation in the early Devonian Rhynie cherts, Aberdeenshire, Scotland. Earth Environ. Sci. Trans. R. Soc. Edinb. 106, 67–80.
Trewin, N.H., Kerp, H., 2017. The Rhynie and Windyfield cherts, early Devonian, Rhynie, Scotland. In: Fraser, N.C., Sues, H.-D. (Eds.), In: Terrestrial Conservation Lagerstätten - Windows into the Evolution of Life on Land. Dunedin Academic Press Ltd, Edinburgh, pp. 1–38.
Tulipani, S., et al., 2015. Changes of palaeoenvironmental conditions recorded in late Devonian reef systems from the Canning Basin, Western Australia: a biomarker and stable isotope approach. Gondwana Res. 28, 1500–1515.
van Schöll, L., Smits, M., Hoffland, E., 2006. Ectomycorrhizal weathering of the soil minerals muscovite and hornblende. New Phytol. 171, 805–816.
van Schöll, L., Kuyper, T.W., Smits, M.M., Landeweert, R., Hoffland, E., van Breemen, N., 2008. Rock-eating mycorrhizas: their role in plant nutrition and biogeochemical cycles. Plant Soil 303, 35–47.
van Straalen, N.M., 2021. Evolutionary terrestrialization scenarios for soil invertebrates. Pedobiologia 87–88, 150753.

Versteegh, G.J.M., Riboulleau, A., 2010. An organic geochemical perspective on terrestrialization. Geol. Soc. Spec. Publ. 339, 11–34.
Volkman, J.K., 2003. Sterols in microorganisms. Appl. Microbiol. Biotechnol. 60, 495–506.
Wacey, D., Kilburn, M.R., Saunders, M., Cliff, J.B., Kong, C., Liu, A.G., et al., 2015. Uncovering framboidal pyrite biogenicity using nano-scale CNorg mapping. Geology 43, 27–30.
Wellman, C.H., 2006. Spore assemblages from the lower Devonian 'lower Old Red Sandstone' deposits of the Rhynie outlier, Scotland. Trans. R. Soc. Edinb. Earth Sci. 97, 167–211.
Wellman, C.H., Graham, L.E., Lewis, L.A., 2019. Filamentous green algae from the early Devonian Rhynie chert. Paläontol. Z. 93, 387–393.